DEVELOPMENT OF NANOFILTRATION MEMBRANES THROUGH SURFACE MODIFICATION OF POLYSULFONE BASED ULTRAFILTRATION MEMBRANES

A Thesis Submitted to
the Graduate School of Engineering and Sciences of
İzmir Institute of Technology
in Partial Fulfillment of the Requirements for the Degree of

MASTER OF SCIENCE

in Chemical Engineering

by
Canbike BAR

December 2017
İZMİR

We approve the thesis of **Canbike BAR**

Examining Committee Members:

_____
Prof. Dr. Sacide ALSOY ALTINKAYA
Department of Chemical Engineering, İzmir Institute of Technology

_____
Prof. Dr. Nalan KABAY
Department of Chemical Engineering, Ege University

_____
Assistant Prof. Ayben TOP
Department of Chemical Engineering, İzmir Institute of Technology

27 December 2017

_____
Prof. Dr. Sacide ALSOY ALTINKAYA
Supervisor, Department of Chemical Engineering
İzmir Institute of Technology

_____
Prof. Dr. Erol ŞEKER
Head of the Department of Chemical Engineering

_____
Prof. Dr. Aysun SOFUOĞLU
Dean of the Graduate School of Engineering and Sciences

ACKNOWLEDGEMENTS

I thank all who in one way or another contributed in the completion of this thesis. First of all, I would like to express my gratitude to my advisor Prof. Dr. Sacide ALSOY ALTINKAYA who for the continuous support of my MSc study and research, for her patience, motivation, enthusiasm, and immense knowledge. Her guidance helped me in all the time of research and writing of this thesis. It has been a great honour to work with her to show the way how to be an honest and productive researcher.

I would also like to thank to my committee members, Prof. Dr. Nalan KABAY and Assistant Prof. Ayben TOP for their valuable suggestions and recommendations to improve the quality of my thesis.

I would like to thank for my close friend, spiritual brother in my life and co-worker Önder TEKİNALP for his supports, stimulating discussions, the sleepless nights when we were working together and for all the fun we have had in the last 3 years. I thank my co-workers Nagehan ÇAĞLAR for her help, support and sleepless nights when we were working together before deadlines throughout the TUBITAK project and Aydın CİHANOĞLU for his support and the stimulating discussions. Also I thank my close friends; Merve UÇAROĞLU for being sister in my life and Ferhat TAMCI for their help and support in daily life whenever I needed and made me think in another way. I feel great luck to know about them!

Furthermore, I am thankful to the Scientific and Technical Research Council of Turkey (TUBITAK, Grant Number: 115M464) for supporting this study.

I would also like to thank to valuable people in Centre for Material Research for their kind help for SEM and AFM analyses and to provide an opportunity to use instruments any time I needed.

Finally, I must express my very profound gratitude to my parents; Leman BAR, Hasan Bar and to my brother; Cantuğ BAR for providing me with unfailing support and continuous encouragement throughout my years of study and through the process of researching and writing this thesis. This accomplishment would not have been possible without them.

ABSTRACT

DEVELOPMENT OF NANOFILTRATION MEMBRANES THROUGH SURFACE MODIFICATION OF POLYSULFONE BASED ULTRAFILTRATION MEMBRANES

Stimuli responsive membranes have been used for suppressing fouling and regulating selectivity in different applications. These types of membranes are usually manufactured in thin film composite structure by either polymerizing stimuli-responsive monomer or coating stimuli-responsive polymer on a support. Responsiveness is due to their characteristic features which rely on reversible changes in mass transfer and interfacial properties as a result of changes in external environment such as pH, temperature and ionic strength.

In this study, a pentablock copolymer (PBC) which consists of temperature responsive Pluronic F127 (PEO-b-PPO-b-PEO) in the middle block and pH responsive poly(N,N-(diethylamino)ethyl methacrylate) (PDEAEM) in the end blocks was used for designing a new type of thin film composite (TFC) nanofiltration membrane. The support of the composite membrane was prepared from a blend of polysulfone/sulfonated polyethersulfone using nonsolvent induced phase separation and the PBC was attached to the support via electrostatic interaction. The conformation of grafted PBC chains was determined by adsorption studies. The effects of PDEAEM block length, concentration of the copolymer and adsorption time on the adsorbed amount were investigated. Among three copolymer samples investigated (15, 20 and 25 kDa), the 25 kDa PBC displayed the highest responsiveness, thus, rejection properties were determined for the membranes prepared only from this sample. The influences of operation pH and temperature on the structure integrity of the membrane were investigated with pure water permeability measurements and the change in pore size was assessed by determining rejection of neutral solutes by the membranes. The membranes were further characterized with SEM, AFM, contact angle, XPS and zeta potential measurements. It was demonstrated that a new pH and temperature responsive, high flux TFC NF membrane was manufactured.

ÖZET

POLİSÜLFON BAZLI ULTRAFİLTRASYON MEMBRANLARINDAN YÜZEY MODİFİKASYONU İLE NANOFİLTRASYON MEMBRANLARININ GELİŞTİRİLMESİ

Dış uyarıcılara tepki veren membranlar, farklı uygulamalarda kirlenmenin önlenmesi ve seçiciliğin düzenlenmesi için kullanılmaktadır. İnce film kompozit membranlar genellikle bir uyarıcıya tepki veren monomerin yüzeyde polimerizasyonu veya uyarıcıya tepki veren bir polimerin yüzeye kaplanması ile üretilmektedir. Dış etkilere duyarlılık, polimerin pH, sıcaklık ve iyonik kuvvet gibi dış ortamdaki değişiklikler sonucunda kütle transferi ve ara yüzey özelliklerindeki değişikliklerden kaynaklanmaktadır.

Bu çalışmada orta blok olarak sıcaklığa duyarlı Pluronik F127 (PEO-b-PPO-b-PEO) ve uç bloklar olarak pH'a cevap veren poli(N, N- (dietilamino) etil metakrilat) (PDEAEM) içeren bir pentablok kopolimer yeni bir ince film kompozit (TFC) nanofiltrasyon membranı tasarımı için kullanılmıştır. Kompozit membranın desteği, polisülfon/sülfonlanmış polietersülfon karışımı ile çözücü olmayan faz ayrımı ile hazırlanmıştır ve PBC, elektrostatik etkileşim yoluyla desteğe tutturulmuştur. Aşılanmış PBC zincirlerinin konformasyonu, adsorpsiyon çalışmaları yoluyla tespit edilmiştir. PDEAEM blok uzunluğu, kopolimer konsantrasyonu ve adsorpsiyon süresinin adsorbe olan PBC miktarı üzerine olan etkileri araştırılmıştır. İncelenen üç kopolimer numunesi (15, 20 ve 25 kDa) arasında pH ve sıcaklığa karşı en fazla cevabı 25 kDa'lık örnek verdiğinden daha sonraki çalışmalarda bu örnekle hazırlanmış membranların PEG tutma özellikleri belirlenmiştir. pH ve sıcaklığın membranın yapısı üzerindeki etkileri, saf su akısı ölçümleri ve nötr bileşiklerin membranlar tarafından tutulma düzeylerinden gözenek boyutundaki değişimi belirleyerek incelenmiştir. Membranlar ayrıca SEM, AFM, temas açısı, XPS ve zeta potansiyeli ölçümleri ile karakterize edilmiştir. Bu çalışmada pH ve sıcaklığa duyarlı, yüksek akıya sahip, yeni bir ince film kompozit nanofiltrasyon membranı üretilebileceği gösterilmiştir.

TABLE OF CONTENTS

LIST OF FIGURES

Figure **Page**

LIST OF TABLES

CHAPTER 1

INTRODUCTION

Membrane separation technology separates the components of the mixture by means of semi-permeable barriers with the help of driving forces such as pressure difference, concentration difference and electrical charge difference. Membrane processes in which pressure difference is used as a driving force are classified as reverse osmosis (RO), nanofiltration (NF), ultrafiltration (UF) and microfiltration (MF) depending on the pore size of the membrane. The pressure applied for reverse osmosis is in the range of 40-80 bar while the lower pressure is applied in the NF process (10-25 bar) which makes it more economical than the RO process (Marcel, 1996). In recent years, the application of NF membranes in effective separation of different streams such as pharmaceuticals, biochemicals and heavy metals have significantly increased (Mulvenna et al. 2014; Bellona et al., 2004; Thong et al., 2014). NF membranes with a pore size of less than 2 nm inhibit the permeation of components with a molecular weight above 1 kDa by 90% (Marcel, 1996). One of the most important challenges for the NF membranes is to achieve this rejection level with a high flux which determines the economics of the NF process.

NF membranes are usually produced in the form of thin film composite (TFC) structure (Thong et al., 2014). These types of membranes are prepared through polymerization of various monomers (grafting from) or coating of previously synthesized polymer (grafting to) on a porous support which provides necessary mechanical strength for the membrane (Ulbricht, 2006). Direct polymerization of monomers on the surface may not take place homogeneously, hence, it is difficult to achieve uniform thickness. Thus, grafting from approach cannot be easily scaled up. On the other hand, physical adsorption can be easily applied and the method can be scaled up for large-scale preparation. In this process, various hydrophilic layers are constructed by dipping or spraying steps or by directly adsorbing water-soluble polymers or stimuli responsive polymers onto membrane surfaces. The main disadvantage of the physical adsorption approach is the instability of the coated layers, which may result in release from the membranes (Zhu et al., 2014).

Different polymers/copolymers have been used in designing selective layer of the TFC membranes. Among these materials stimuli-responsive polymers receive increasing attention due to their ability in responding to external stimuli such as pH, temperature, ionic strength by changing their conformation. The responsive membranes were usually prepared for size-based separations in MF or UF processes (Chen et al., 2013; Nunes et al., 2011; Shevate et al., 2016; Liu et al., 2016).

On the other hand, there are only a few studies on the development of TFC responsive NF membranes (Wu et al., 2017; Himstedt et al., 2013; Yang et al., 2013; Himstedt et al., 2011). Himstedt et al. (2013, 2011) modified the surface of commercial polyamide and NF 270 nanofiltration membranes with polyacrylic acid (PAA) nanobrushes through a UV initiated graft polymerization method. Although glucose is a smaller molecule than sucrose, its rejection was found more than that of sucrose at pH values above the pKa when PAA chains are deprotonated. Yang et al. (2013) grafted poly(2-hydroxyethyl methacrylate) (polyHEMA) chains to the surface of commercial thin film composite nanofiltration membrane through atom transfer radical polymerization. They have demonstrated that polyHEMA chains respond to magnetic field by reporting both increased permeate fluxes and increased salt rejection in the presence of an oscillating magnetic field. The common feature of these studies is the single responsiveness of the membranes. Dual or multiple responsive membranes were prepared in recent studies however they are all in UF category (Chen et al., 2014; Chen et al., 2014; Li et al., 2013; Birkner and Ulbricht, 2015; Xiao et al., 2014). In the case of single responsive membranes, the increase in flux is accompanied with the decrease in the fouling resistance when the hydrophilic segments become hydrophobic in response to stimuli (He et al., 2013).

The objective of this thesis study is to prepare a dual responsive TFC NF membrane. For this purpose, a pentablock copolymer (PBC) which consists of temperature responsive Pluronic F127 (PEO-b-PPO-b-PEO) in the middle block and pH responsive poly(N,N-(diethylamino)ethyl methacrylate) (PDEAEM) in the end blocks formed the selective layer of the composite membrane. The support of the composite structure was prepared from a blend of polysulfone/sulfonated polyethersulfone through nonsolvent induced phase separation and the PBC was attached to the support through electrostatic interaction. The adsorption of PBC with different molecular weights was followed to determine suitable coating conditions so that copolymer is grafted in brushed conformation. The membranes were by using with scanning electron microscopy, atomic

force microscopy, X-ray photoelectron spectroscopy, contact angle and zeta potential measurements. The influences of pH and temperature on the pure water permeability, molecular weight cutoff and pore size of the membranes were investigated. In addition, the reversibility of the responsiveness and pH stability of the membranes were evaluated. To the best of our knowledge this is the first study which uses a dual responsive copolymer in the manufacture of TFC NF membrane and investigates the effect of responsiveness not only on the water flux and rejection but also on the molecular weight cutoff value of the membranes.

This thesis consists of five chapters. After Chapter 1, a literature review was given in Chapter 2 to obtain a comprehensive understanding of the basics of NF process, TFC membranes and stimuli responsive polymers. Experimental protocols used for membrane preparation, characterization, flux and rejection measurements were discussed in Chapter 3. Results were presented and discussed in Chapter 4 and overall conclusions were given in Chapter 5.

CHAPTER 2

LITERATURE REVIEW

2.1. Membrane Separation Process

A membrane is a selective barrier that allows the passage of certain constituents and retains others found in the feed stream (Cheryan, 1998). Membrane technology developed in the 1960s is preferred in many different industries for purification since it is considered as an environmentally friendly process and its application is easy (Mulder, 1997). Figure 2.1 shows a typical membrane separation process.

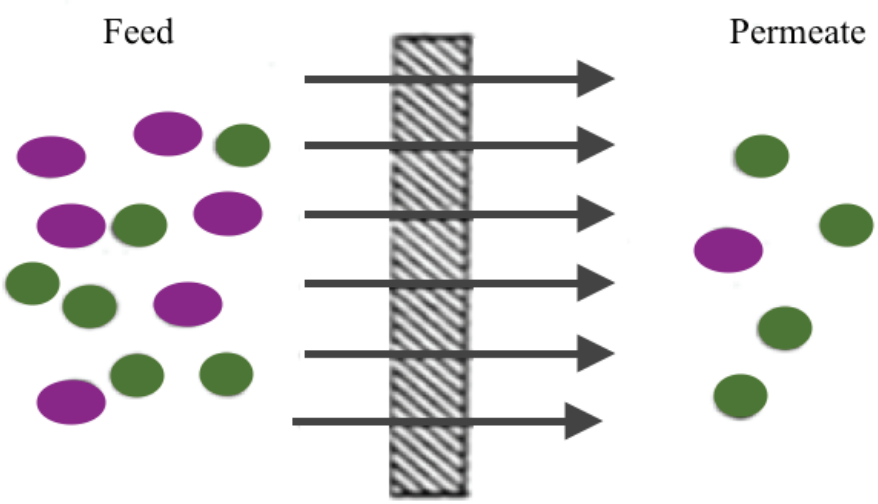

Figure 2.1. Schematic representation of membrane separation process.
(Source: Reprinted with permission from Pinto et al., 1999)

2.2. Driving Forces for Membrane Separation Processes

Membrane separation is carried out with different driving forces such as electrical potential difference, concentration difference, temperature difference and pressure difference (Mulder, 1996). In pressure-driven membrane processes, the feed stream is separated into retentate and permeate by means of the pressure exerted on the feed stream (Van der Bruggen, 2003). Membranes operated with the pressure difference are classified as reverse osmosis (RO), NF, UF and MF. As seen from Figure 2.2, the pressure

difference applied decreases from 30-60 bar in RO down to < 1 bar in MF membranes as a result of increase in average pore size, the smallest pores exist in RO membranes while the largest pores are found in MF membranes.

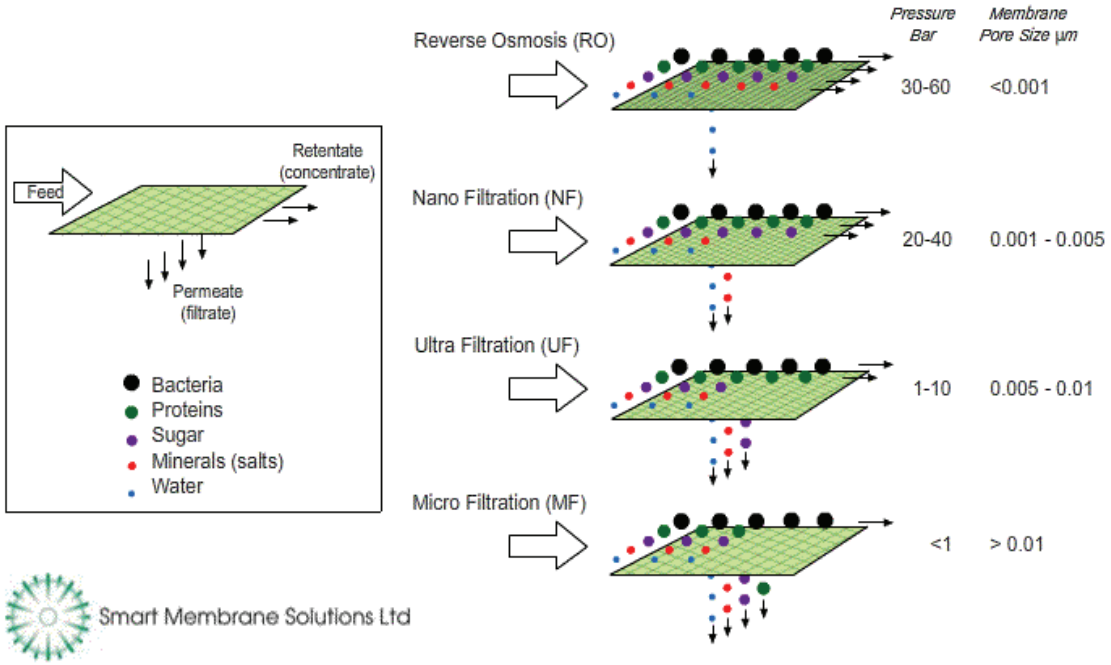

Figure 2.2. Types of pressure driven based membrane processes.
(Source: Taken from http://www.smartmembranesolutions.co.nz/membrane-classifications/ Accessed in November, 2017)

2.3. NF Process

NF membranes have average pore sizes between UF and RO membranes and require lower pressure, thus, lower energy consumption than RO which make this process suitable for removal of relatively small organics such as sugar, dye, and metals etc. (Van der Bruggen, 2003). For commercial NF membranes, the average pore size and molecular weight cutoff (MWCO) range between 1 nm and 10 nm for 200 Da and 1,000 Da, respectively (Boussu et al., 2006). NF covers a wide range of applications like water softening, wastewater treatment, recovery of valuable compounds and removal of heavy metals. NF membranes are prepared either by a single step phase inversion or in the form of a TFC structure. Phase inversion usually results in micron sized pores in the sublayer of the membrane, although pores on the surface are smaller than in the bulk, their sizes are still large compared to the sizes required for NF process. It is easier to obtain desired pore sizes for NF with TFC membranes since the structure is made from 2 distinct layers.

2.4. TFC Membrane

TFC membranes consist of at least two layers that are ultrathin selective layer and porous support layer as shown in Figure 2.3 (Mulder, 1996).

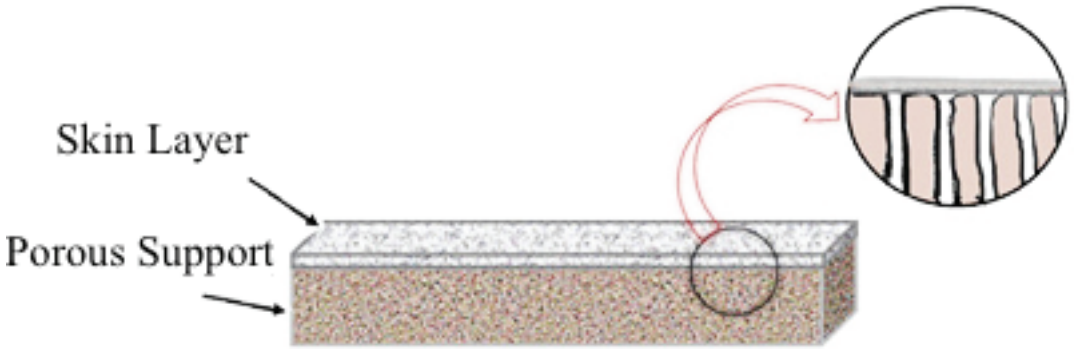

Figure 2.3. TFC membrane structure.
(Source: Taken from http://www.ctamgu.in/membrane.html Accessed in November, 2017)

Generally, porous support membrane is prepared by phase inversion method. The selective layer on the porous support is formed by various techniques including plasma polymerization, dip coating, in situ polymerization, and interfacial polymerization (Mulder, 1996; Lau et al, 2012). Among these techniques, dip coating allows uniform deposition of selective layer even if the coated area is large, thus, the method can be easily scaled up.

The first stage of TFC membrane manufacturing process is the preparation of the porous support layer by phase inversion. This method involves casting polymer solution onto a nonwoven fabric or glass support and immersing it in a non-solvent coagulation bath as shown in Figure 2.4. In coagulation bath, homogeneous solution separates into polymer lean and polymer rich phases. Figure 2.5 shows that the concentration of initial polymer solution which consists of polymer and solvent changes when immersed in the coagulation bath. Once the polymer solution crosses the binodal line phase separation takes place. The rate of phase inversion can be controlled by changing either casting and coagulation conditions such as solvent type, polymer concentration, additives, casting thickness, coagulation bath composition or temperature and pre-evaporation time.

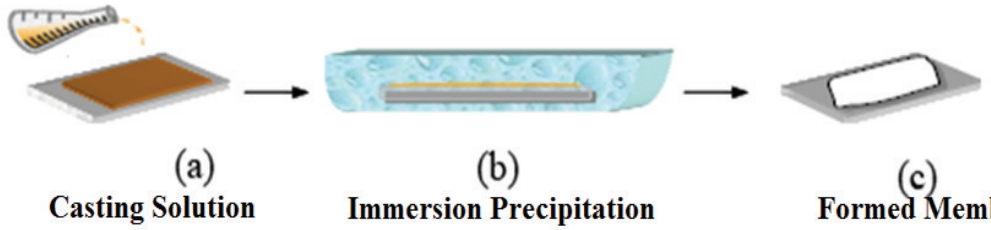

Figure 2.4. Schematic representation of a membrane preparation process by phase inversion technique. (Source: Reprinted with permission from Algieri et al., 2014)

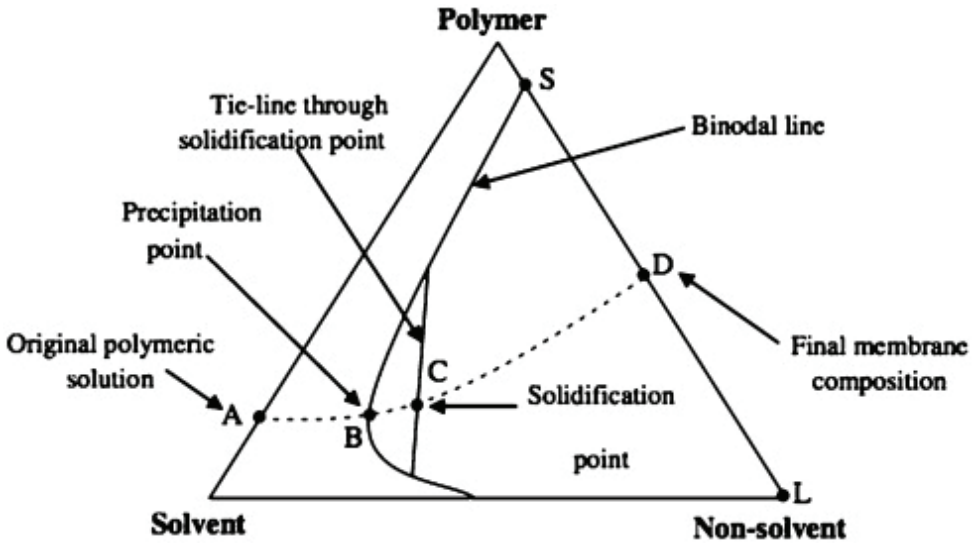

Figure 2.5. Ternary phase diagram of polymer, solvent and nonsolvent. (Source: Reprinted with permission from Jamil et al., 2015)

2.5. Stimuli Responsive Membranes

Stimuli-responsive membranes play an important role in membrane technology. They exhibit distinct property variations as a response to external changes in their environment such as temperature, pH, ionic strength, light, electric and magnetic fields, and chemical cues (Liangyin et al., 2011; Wandera et al., 2010). These types of membranes were developed based on a biomimetic approach. Living cell membranes constitute pore-forming proteins which act as ion channels. Such stimuli-responsive biomembranes provide an exciting model for membrane scientists and technologists to develop smart membranes. Stimuli responsive membranes can be developed as smart hydrogel membranes or smart membranes with grafted stimuli-responsive surfaces and stimuli responsive gates (Figure 2.6).

Surface modification of membranes with stimuli responsive polymers are carried out by grafting or coating onto the membrane surface. Functional polymers that have free mobile ends give flexibility of conformational change on the membrane surface. Membrane performances such as pure water permeability and hydrophilicity and MWCO/average pore size can be controlled by the environmental conditions.

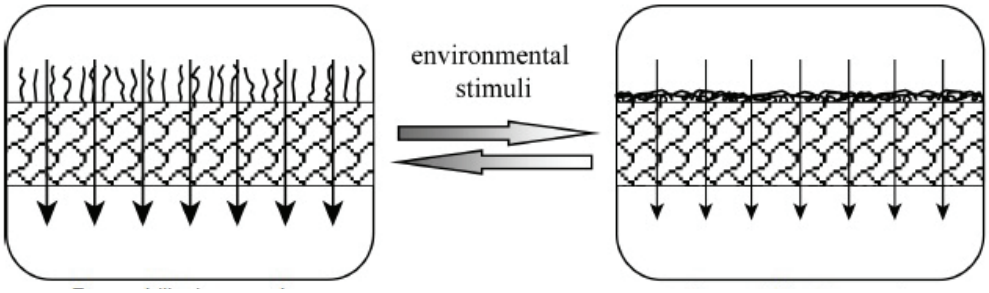

Figure 2.6. Stimuli-responsive smart membrane with grafted responsive surface.
(Source: Reprinted with permission from Liangyin et al., 2011)

2.5.1. Conformation of Polymer Chains

The molecular brush is a special type of graft copolymer in which the polymer chains are grafted with a linear polymer, that is, only one end of the polymer chain is held on the surface (Lee et al.; 2010). The molecular brush can be seen in two different conformations. First one is mushroom structure and second one is brush-like structure.

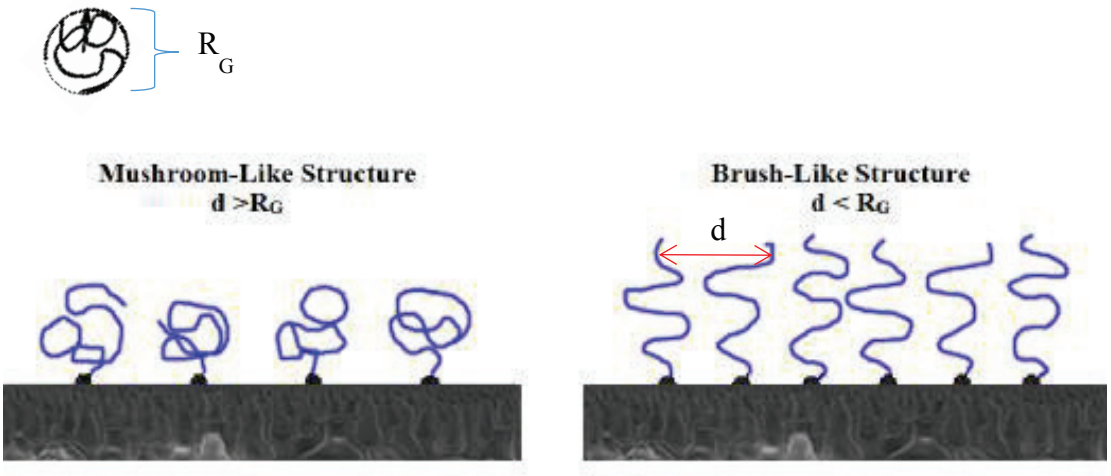

Figure 2.7. Conformation change of responsive polymers.
(Source: Drawn on the basis of Lee et al., 2010)

In Figure 2.7, d represents distance between the interaction points and R_G is the radius of gyration of the polymer that is the distance between end points of the polymer. When the $d>R_G$, mushroom structure is observed. Oppositely, when $d<R_G$, brushed conformation is observed. Chain conformation determines selectivity and antifouling property of TFC membranes (Zhou et al., 2016).

2.5.2. pH Responsiveness

pH responsive polymers have ionizable functional groups which are capable of donating or accepting protons with a pH change (Liangyin, 2011; Liu and Urban, 2010). Membrane pore size can be continuously adjusted by changing pH and it also affects the membrane separation performance. When the pH of the solution is below its pKa value, the carboxylic acid groups are protonated leading to decreased hydration and are in a compact, collapsed form. As the pH increases above the pKa, the carboxylic acid groups become deprotonated and repel each other (Davrishmanesh et al., 2015; Lee et al., 2010). In this case, electrostatic repulsions between generated charges cause fully stretched conformation. In Figure 2.8, the conformation change can be seen.

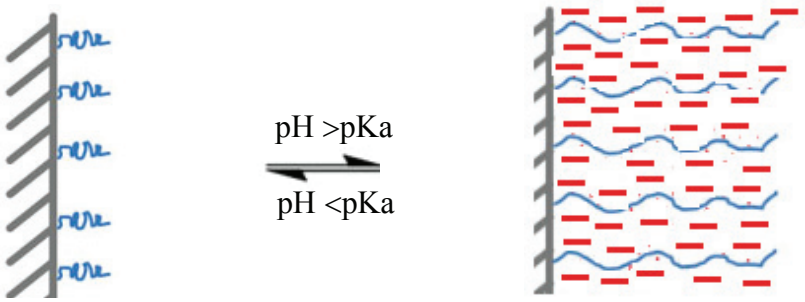

Figure 2.8. Conformation change of carboxylic acid groups according to pH change. (Source: Drawn on the basis of Davrishmanesh et al., 2015)

On the other hand, pyridine groups are deprotonated when the pH of the solution is above its pKa. The conformation of polymer is in compact, collapsed form. As the pH decreases below the pKa, the pyridine groups are protonated and become positively charged (Davrishmanesh et al., 2015). In this case, electrostatic repulsions between generated charges cause fully stretched conformation (Figure 2.9).

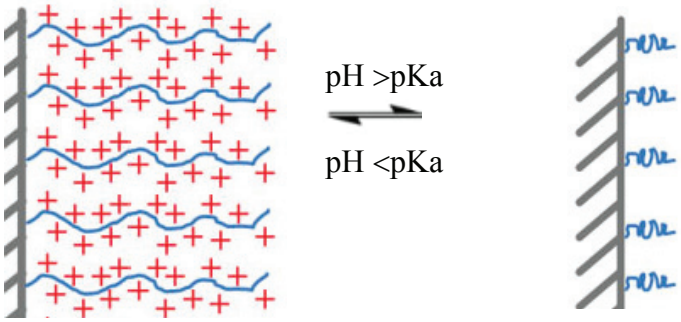

Figure 2.9. Conformation change of pyridine groups according to pH change. (Source: Drawn on the basis of Davrishmanesh et al., 2015)

Himstedt et al. (2011) studied the effect of pH responsiveness of polyacrylic acid (PAA) nanobrushes on the rejection of glucose. The pKa value for PAA is 4.25. They found that the rejection of glucose was highest at pH 7.25 and lowest at pH 3.15. At pH 7.25 it was expected that these nanobrushes are deprotonated and swollen. In this form PAA nanobrushes tend to reduce the size of the membrane pores. In another example, pH responsive PAA nanochains were used to modify the surface of commercial NF270 membranes by using UV initiated free radical polymerization. They found that permeate flux was dependent on feed pH which also adjusted the chain conformation of PAA nanochains. The rejection of two model sugars, glucose and sucrose, was also changed with changing pH of the feed (Himstedt et al., 2013).

The reversible change of membrane properties was investigated by Wang and his group (2017). Polysulfone-graft-poly(4-vinylpyridine) (PSF-g-P4VP)-blended PSf membrane was prepared and switching properties were investigated by analyzing pure water permeability change with pH. They showed that the membrane flux can be changed with changing pH of the environment (Figure 2.10). In addition, they proved that changing pH also affected the meso-tetraphenylsulfonato porphyrin (TPPS) rejection. Another group studied PVDF and PVDF-g-PMAA blend membranes to determine the reversibility of water flux and the effect of pH on the rejection of BSA. They observed strong pH responsiveness (Yang et al., 2017).

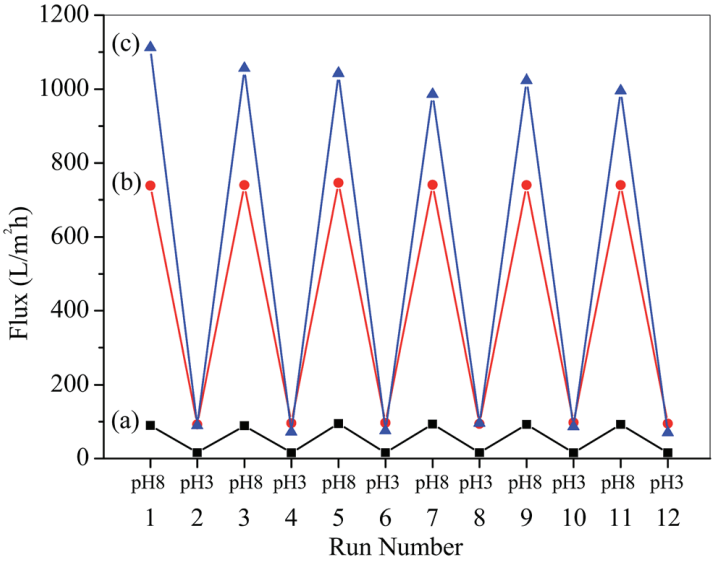

Figure 2.10. Reversible change of pure water flux.
(Source: Taken from Wang et al., 2017)

2.5.3. Temperature Responsiveness

Temperature-responsive polymers are polymers that exhibit a change of their chain conformation with temperature. Membrane pore size, MWCO and pure water permeability (PWP) can be controlled by changing temperature above or below the lower critical solution temperature (LCST). The critical temperature separates the miscible and immiscible region of polymers (Lee et al.; 2010).

When the temperature is increased above the LCST, the polymer becomes immiscible/insoluble in water and the conformation of polymer is in compact, collapsed form. As a result, the size of polymer coils and the pore size of the membrane increases. On the other hand, when the temperature is reduced below the LCST, the polymer becomes miscible/soluble and fully stretched conformation can be observed and the pore size of the membrane decreases (Asatekin and Mayes, 2009). Poly(N-isopropylacrylamide) (PNIPAAm) is the mostly used temperature responsive polymer which has a LCST of 32^{o}C. Temperature responsiveness of PNIPAAm was studied by different research groups using derivatives of PNIPAAm polymer chains. When the temperature is below the LCST, there is an attraction between the PNIPAAm chain and large amount of water molecules is attracted through hydrogen bonding. At this condition, they are in a swollen and hydrophilic state. In contrast, when the temperature is higher than the LCST the PNIPAAm is dehydrated and as a result they are in a collapsed, hydrophobic state (Liangyin et al., 2011; Davrishmanesh et al., 2015).

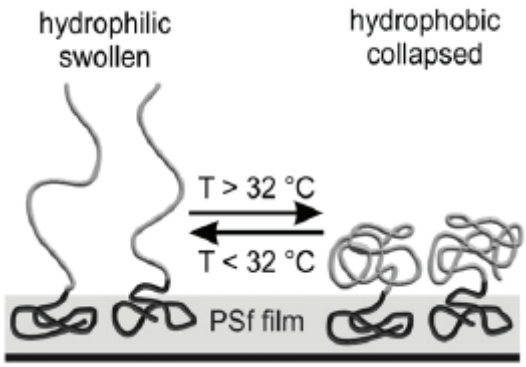

Figure 2.11. Conformation change of surface functionalization by a block copolymer composed of a temperature responsive functional block. (Source: Reprinted with permission from Berndt and Ulbricht, 2009).

Asatekin et al. (2009) studied temperature responsive polymer, poly(vinylidene fluoride) with poly(oxyethylene methacrylate) (PVDF-g-POEM) to adjust pore size by changing environmental conditions. They used reactive red 120 (RR) dye solution for rejection experiments. Increasing the temperature increased the amount of RR passed through the membrane. When the temperature approached the LCST the rejection decreased which indicated the enlargement of pores.

2.5.4. Dual Responsiveness

Polymer production with dual responsive properties has an important potential in technological development. The most widely used dual responsive polymers are obtained by combining temperature and pH (Lee et al., 2010). Yi et al. (2010) studied the performance of the membranes prepared with polyether sulfone (PES) blended with pH and temperature sensitive polymer chain containing F127(PEO-b-PPO-b-PEO) and poly(N,N–dimethylamino-2-ethyl methacrylate) (PDMAEMA) amphiphilic block copolymers (F127-b-PDMAEMAn). Unlike middle block, end groups of the polymer have both pH and temperature responsiveness. To determine the pH effect on the membrane performance, the solution pH was increased from 2.5 to 12.5. The polymer chains at lower pH values are in extended form due to the protonation. On the other hand, polymer chains collapsed at lower pH due to the deprotonation. Consequently, increasing pH value increased the water flux and also the sensitivity of the chains to pH was increased by increasing the degree of polymerization. Membranes prepared with F127-b-$PDMAEMA_{225}$ as an additive showed 2.2 times increment in membrane performance

when pH was increased from 2.5 to 10.5 (Figure 2.12). Additionally, reversible water flux was also observed for the membranes prepared with temperature responsive polymers (Figure 2.12 and Figure 2.13).

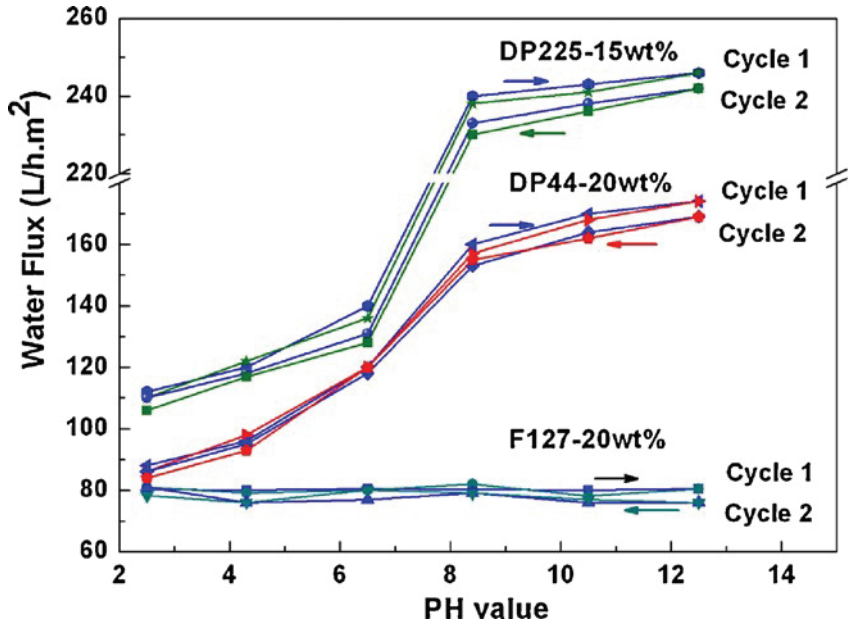

Figure 2.12. Two cycle water flux with different solution pH. (DP: polymerization degree of PDMAEMA blocks; temperature: 25ºC; →: pH increase; and ←: pH decrease). (Source: Reprinted with permission from Yi et al., 2010)

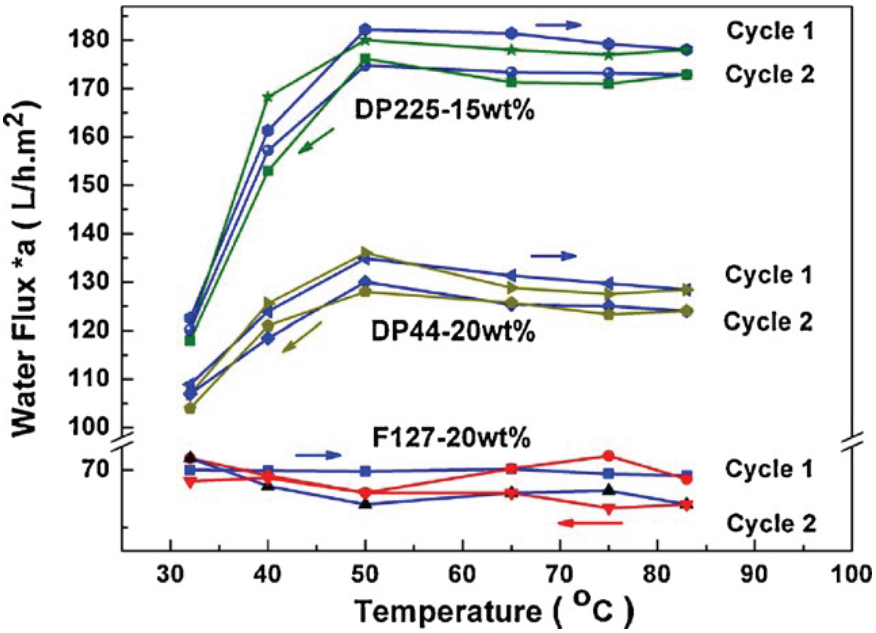

Figure 2.13. Two cycle water flux with different solution temperature. (DP: polymerization degree of PDMAEMA blocks; →: temperature increase; and ←: temperature decrease). (Source: Reprinted with permission from Yi et al., 2010)

Tomicki et al. (2011) studied the performance of surface-functionalized poly(ethylene terephthalate) (PET) membranes with pH and temperature responsive PDMAEMA polymer. Polymer grafting density was investigated on the membrane performance at different pH and temperature. Permeability of the prepared membranes was reduced with decreasing temperature and pH parameters separately due to the conformation of chains.

CHAPTER 3

MATERIALS AND METHODS

3.1. Materials

Polysulfone (PSf) with a molecular weight 35 kDa from Sigma Aldrich Co. and sulfonated polyethersulfone (SPES) with a molecular weight of 80 kDa from Konishi Chemicals, Japan were used in the preparation of the porous support membrane. As solvents, 1-methyl-2-pyrrolidone (NMP) and N,N-Dimethylacetamide (DMAc) with respective purities of >99.5% and >99% were purchased from Sigma Aldrich and used to dissolve PSf and SPES. For support optimization sodium dodecyl sulfate (SDS) and TWEEN 80 were used and they were purchased from Sigma Aldrich. Alginic acid sodium salt from brown algae (ALG) with the range of molecular weight of 80-120 kDa and polyethyleneimine (PEI) with a average molecular weight of 25 kDa were supplied by Sigma Aldrich and used as polyelectrolytes to produce TFC membrane. Sodium hydroxide (NaOH) in pellets and hydrochloric acid (HCl) 37% were also purchased from Sigma Aldrich, USA and used to adjust the solution pH. Polyethylene glycol (PEG) with molecular weights of 600/1000/6000/10000 Da, glycerol, glucose and sucrose were purchased from Sigma Aldrich and used for filtration tests.

Figure 3.1 shows the structures of the polymers, PSf, SPES, PEI, ALG and PBC, used in the preparation of TFC membrane. The numbers of PDEAEM monomers (n) of the 15, 20 and 25 kDa PBC molecules were 2, 9 and 15, respectively.

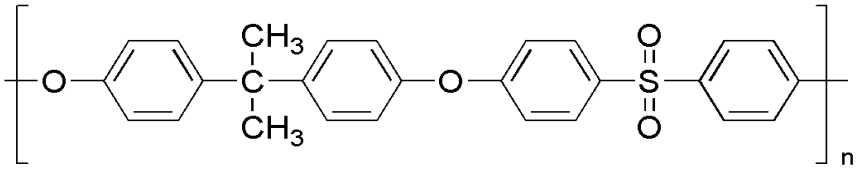

(a)

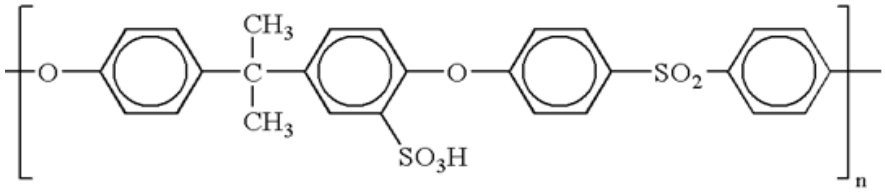

(b)

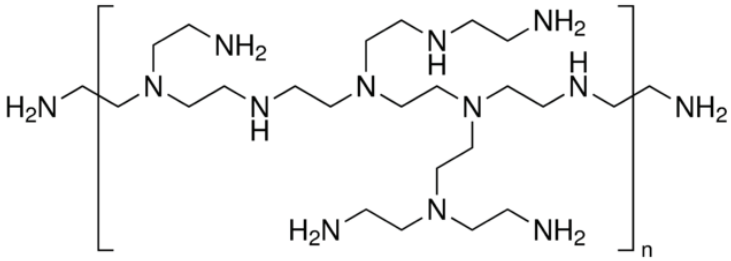

(c)

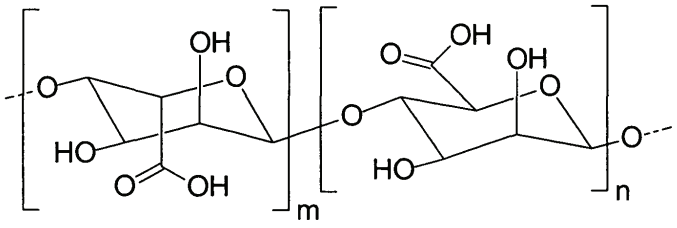

(I)

(d)

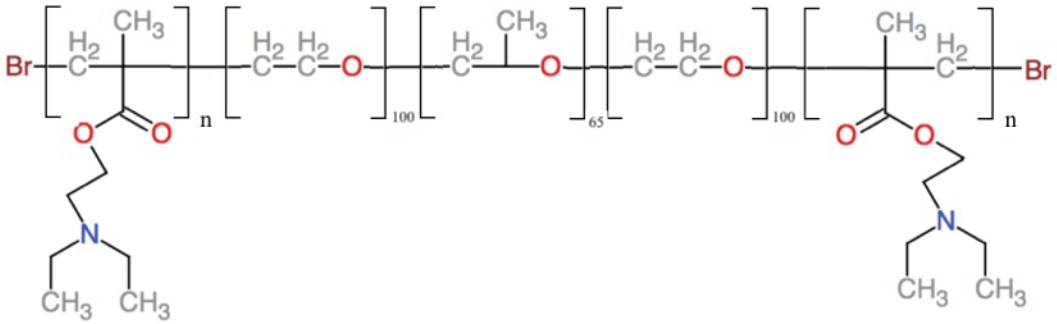

(e)

Figure 3.1. Structure of polymers (a) PSf (b) SPES (c) PEI (d) ALG (e) PBC.

3.2. Membrane Preparation

The porous support layer of the TFC membrane was prepared from a blend of PSf and SPES polymers. Firstly, polymers were dried for 24 h at 80°C under vacuum. Then, 25 wt% polymer in (1:3) ratio of SPES:PSf and 75 wt% solvent in (1:2) ratio of NMP:DMAc were mixed for 24 h at 100 rpm until homogeneous solution was obtained. After complete dissolution, nonwoven fabric (purchased from HIROSE Paper Co.; Product Code: 05TH-100) was taped on the glass plate and the solution was poured onto a nonwoven support with a casting knife having a 250 μm gate size at room temperature. The polymer solution was then immediately immersed into a coagulation bath containing 0.5 wt% PEI solution at 25°C. After coagulation, each membrane was kept in the PEI solution for 12 h and washed ~3 days with deionized (DI) water to remove excess PEI on the surface and finally stored in DI water until the filtration tests.

To prepare TFC membrane, porous support membrane was first modified with 1 mg/mL alginate solution at pH 4. The modification was performed by filtering ALG solution at 1 bar for almost 15 min using a dead-end filtration cell (Model 8010, Millipore Corp.). After the filtration, the membrane surface was rinsed 5 times and washed with DI water for 5 min to remove loosely bound ALG. Next, the DI water at pH 4 was permeated through the membrane at 2.5 bar until steady state is reached. Afterwards, the PBC solution with a pH adjusted to 4 was filtered through ALG modified support membrane at 1 bar for 120 min.

3.3. Adsorption Kinetics of PBC

The PBC with three different molecular weights (15, 20, 25 kDa) used in this thesis were synthesized using atom transfer radical polymerization by Prof. Mallapragada's group in Chemical and Biological Engineering Department at Iowa State University in USA. The experimental setup used for determining adsorption kinetics of PBC was shown in Figure 3.2. The support membrane modified with ALG under dynamic conditions was placed between two rubber pieces. The PBC solution was dropped onto membrane surface. The volume of PBC solution was used as 600 μl and the area of the membranes was fixed at 2x1 cm^2. To prevent evaporation, the surface was covered with a rubber lid. At the end of 1 h, 2 h, 4 h, 6 h, 12 h and 24 h, the solution was removed

from membrane surface and then the membrane was washed with DI water to prevent loosely bound PBC. Then these TFC membranes were dried under room conditions for 48 h. Finally, their weights were measured with an electronic balance (Sartorius CP2P, Germany; max. weighing capacity: 2.1 g; readability: 0.001 mg). Dry weight of the alginate-modified membranes was also measured. Amount of PBC adsorbed (A_d) on the surface was then determined by the following equation:

$$A_d = m_{ALG/PBC\ coated\ membrane} - m_{ALG\ coated\ membrane} \quad (3.1)$$

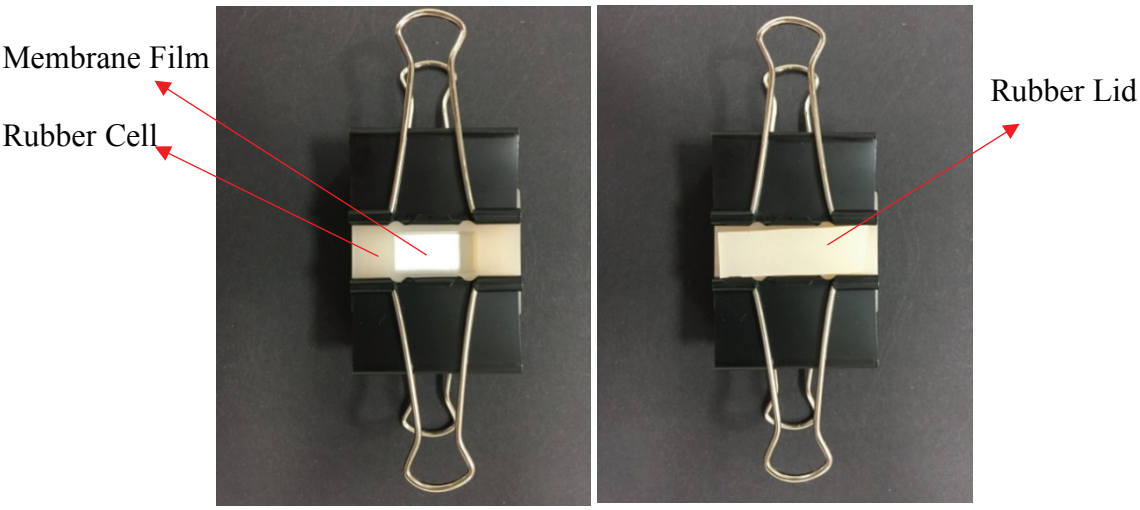

Figure 3.2. Experimental setup used for determining adsorption kinetics of PBC.

The concentrations of the copolymer (6, 8, 12 and 18 mg/mL) were chosen under its critical micelle concentration (Determan et al., 2006) to prevent micellization of the chains before adsorption. The block copolymer was attached to the support membrane via electrostatic interaction between positively charged amine groups and negatively charged alginate. It is desirable to attach only one end of the copolymer in brushed conformation in order to achieve maximum benefit from both pH dependent hydrophilic character and anticipated antibacterial property of PDEAEM groups.

3.4. Filtration Experiments

3.4.1. Water Flux Measurement

Water flux tests were carried out using a dead-end cell filtration system (Model 8010, Millipore Corp.) with a total internal volume of 10 mL and active surface area of 4.1 cm^2. Delivery of feed solution to the cell was provided by a stainless-steel dispensing pressure vessel (Millipore) pressurized with a nitrogen cylinder. To simulate the flow conditions in an actual filtration, the magnetic stirrer was used to obtain a homogeneous solution during filtration as shown in Figure 3.3. In the experiments, a circular flat sheet membrane was cut and placed into membrane holder. After mounting in the filtration cell, each membrane was first compacted by filtration of DI water with pH 4 at the compaction pressure (2.5 bar) to reach steady state flux. After the compaction procedure, the pressure vessel was closed and the cell was successively emptied from nitrogen gas. Then, filtration cell was filled with DI water at pH 4.0 and the flux measurements were performed at room temperature with a stirring speed of 500 rpm and measurement pressure (P_m) of 2 bar for approximately 45 min. Then, flux was calculated from volume vs time graph. The flux J_w (L/m^2h) and the PWP of the membranes were calculated by the following equations:

$$\mathrm{Jw} = \left(\frac{\Delta \mathrm{V}}{A\ x\ \Delta \mathrm{t}}\right) \tag{3.2}$$

$$\mathrm{PWP} = \left(\frac{\Delta \mathrm{V}}{A\ x\ \Delta \mathrm{t}\ \mathrm{x}\ \Delta \mathrm{P}}\right) \tag{3.3}$$

where ΔV is the volume of permeated distilled water (L), A (m^2) is the membrane area, Δt (h) is the permeation time and ΔP (bar) is the transmembrane pressure difference applied through the membrane. The experiments were carried out at 4 and 25°C.

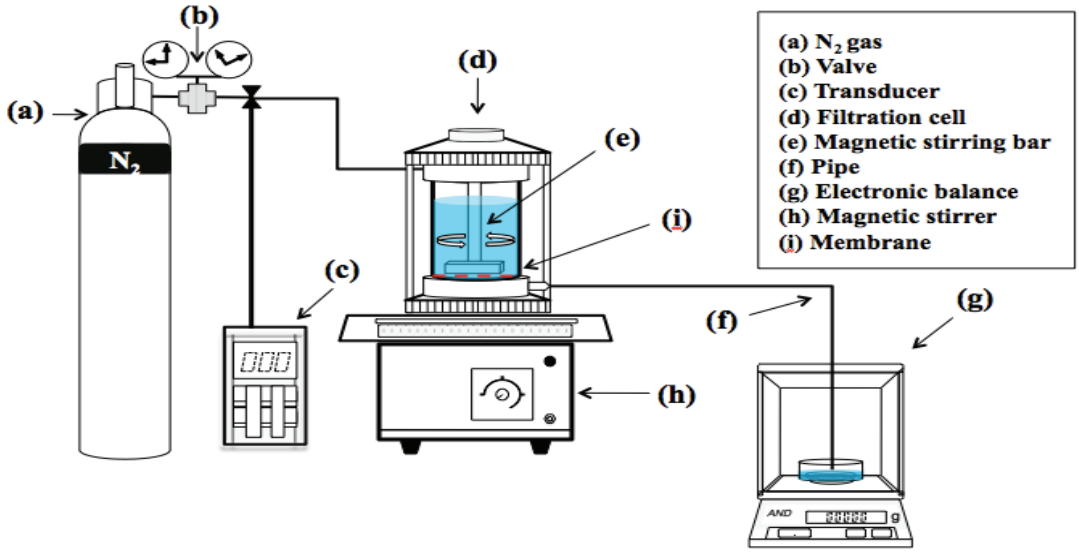

Figure 3.3. Dead-end filtration unit.
(Source: Taken from
http://www.intechopen.com/source/html/37613/media/image26.png">Intechopen.com
Accessed in November, 2017)

3.4.2. Rejection Measurement

Filtrations of model solutes were carried out in the same dead-end filtration cell system as described above under different conditions as listed in Table 3.1.

Table 3.1. Parameters of filtration experiments.

pH of the feed solution (at 25°C)	4.0
	7.6
	8.5
Temperature of the feed solution (at pH 7.6)	4°C
	25°C

Before rejection experiments, pure water was filtered through the membranes. Then, the feed solutions with 1 g/L of concentration were prepared by dissolving neutral solutes [polyethylene glycol (PEG) (Mw=600 Da, 1000 Da and 6000 Da), sucrose (Mw=342 Da), glucose (Mw=180 Da) and glycerol (Mw=92 Da)] in DI water. The pH of feed solution was adjusted with NaOH or HCl. During the experiment first 10 mL of feed solutions were filled into the cell. After filtration of 5 mL, the remaining 5 mL were kept as retentate solution. Upon changing the feed solution, membrane was rinsed five times with DI water and 10 mL DI water was filtered through the membrane to ensure

that the permeability of the membrane did not change after neutral solute filtration. The concentrations of solutes in feed solution (C_f), permeate (C_p) and the retentate (C_r) were determined using Rudolph - J357 mode automatic refractometer. The rejection was calculated by using formula given below.

$$R\ (\%) = \left(1 - \frac{C_p}{C_{avg}}\right) x100 \tag{3.4}$$

$$C_{avg} = \frac{C_f + C_r}{2} \tag{3.5}$$

3.5. Characterization of the Membranes

3.5.1. Scanning Electron Microscopy (SEM)

SEM (FEI Quanta 250 FEG) was used for characterization of the membrane cross-sectional morphology. Membrane samples were prepared by cracking by using liquid nitrogen. Dried samples were coated with gold by using Magnetron Sputter Coating Instrument, prior to analysis.

3.5.2. Atomic Force Microscopy (AFM)

AFM analysis was performed in dry condition by using MMSPM Nanoscope 8 from Bruker. Scanning was performed with dried membranes in tapping mode for 5x5 μm^2 surface using TAP150 model tip (material: 0.01-0.025 Ohm-cm Antinomy (n) doped Si).

3.5.3. Contact Angle

The hydrophilic character of control and TFC membranes was analyzed with static contact angle measurements by Attension Optical Tensiometer. Before experiment, membranes were dried for 24 h at room temperature to remove the moisture. Samples were attached to the microscope slide by a double-sided tape. Measurements were carried

out at ambient temperature, 30 sec after 5 µl of DI water at different pH (4.0, 7.6, 8.5) and temperature (4, 25°C) was dropped on the surface.

3.5.4. X-Ray Photoelectron Spectroscopy (XPS)

XPS analysis of support and 25 kDa coated membranes was performed to confirm the presence of PBC coating and also to determine the conformation of attached copolymer chains using Thermo Scientific K-Alpha model. The experiments were carried out with an electron takeoff angle between 0 and 45° to the sample plane. Also, the brushlike configuration of PBC was confirmed by depth profile method.

3.5.5. MWCO and Average Pore Size Determination

The influences of pH and temperature on the pore size of the membranes were determined through measuring rejection of model neutral solutes by the membranes. The pore sizes were evaluated by using experimentally measured rejection data and Equations 3.6 through 3.10 (Deen, 1987; Bowen and Mohammed, 1998)

$$R = 1 - \frac{C_p}{C_{avg}} = 1 - \frac{K_{i,c}\Phi}{1-\exp(Pe_m)[1-\Phi K_{i,c}]} \qquad C_{avg} = \frac{C_f+C_r}{2} \tag{3.6}$$

$$Pe_m = \frac{K_{i,c}}{K_{i,d}}\frac{V\,L}{D_{i,\infty}\,A} \qquad \Phi = (1-\lambda)^2 \qquad \lambda = \frac{r_s}{r_p} \tag{3.7}$$

$$K_{i,d} = K^{-1}(\lambda, 0) \qquad K_{i,c} = (2-\Phi)G(\lambda, 0) \tag{3.8}$$

$$K^{-1} = 1 - 2.401\lambda + 1.153\lambda^2 - 0.118\lambda^3 \tag{3.9}$$

$$G(\lambda, 0) = 1 + 0.042\lambda - 0.941\lambda^2 + 0.339\lambda^3 \tag{3.10}$$

In these equations C_p and C_{avg} represent the solute concentrations in permeate and feed streams, V is the filtration rate, L and A are the membrane thickness and porosity, $D_{i,\infty}$ is the solute diffusivity in solution, λ is the ratio of solute pore size to average pore size, and r_s and r_p are the solute and pore sizes.

3.6. Stability and Reversibility of Responsiveness

The stability of the layers on the membrane surface was investigated by storing the membranes in DI water at pH 4.0 and 8.5 under static conditions. The pure water permeability and PEG 1000 rejection of the membranes were measured before and after 30 days of storage in DI water. The reversibility of conformation of chains was determined by alternately switching the solution pH between 4.0 and 8.5 and solution temperature between 4ºC and 25ºC and measuring PWP at these conditions.

CHAPTER 4

RESULTS AND DISCUSSION

In TFC NF membranes, the rejection properties are mainly determined by the selective layer. On the other hand, the morphology of the support membrane has also an influence on the rejection and permeability of the composite structure. In the following section, the results of the optimization of support membrane preparation were discussed. Then, the results of adsorption kinetics of PBC and the TFC membranes were presented.

4.1. Support Membrane Preparation Without Nonwoven Fabric

4.1.1. Effect of Coagulation Bath Temperature

The coagulation bath temperature influences the final membrane morphology because of its effect on the rate of phase separation. Membrane is formed by immersing a polymer solution that consists of polymer and solvent (S) into a coagulation bath containing a nonsolvent (NS) usually DI water. During immersion, solvent diffuses towards the coagulation bath while NS diffuses into the polymer solution. At one point, the cast solution becomes thermodynamically unstable and separates into polymer lean and polymer rich phases. Finally, demixing occurs and solid polymeric film is obtained (Mulder, 1996). By changing temperature of the coagulation bath, the rate of exchange of S and NS is adjusted. Table 4.1 shows the influence of coagulation bath temperature on the PWP and PEG 6000 rejection of the membranes.

By changing the coagulation bath temperature from 25 to 4^{o}C the PWP of the support membrane slightly decreased while PEG 6000 rejection increased by a factor of 3.75. This can be explained by delayed demixing rate as a result of slower diffusion of both S and NS resulting in in smaller voids (Amirilargani et al., 2010). By considering significant increase in PEG 6000 rejection and only slight decrease in PWP, it was decided to set coagulation bath temperature at 4^{o}C.

Table 4.1. The effect of coagulation bath and storage temperature on the membrane performance.

	Storage T: 25°C Coagulation Bath T: 20°C	Storage T: 4°C Coagulation Bath T: 4°C
PWP ($L/m^2.h.bar$)	144 ± 4.74	103 ± 0.86
PEG 6000 Rejection (%)	12 ± 3.05	45 ± 9.8

**The support membrane was cast with 25% polymer concentration (PSf:SPES ratio: 4); casting thickness: 250 μm; coagulation bath: DI water; immersion time: 10 min.

4.1.2. Effect of PSf:SPES Ratio

Figure 4.1 illustrates that the PWP of support membrane increased by increasing the PSf:SPES ratio from 3 to 4. However, further increase in the ratio dramatically decreased the PWP due to hydrophobic character of PSf. Increasing the PSf:SPES ratio from 4 to 5.67 significantly enhanced the PEG 6000 rejection from 55% to 100%. Similar results were also reported by Jacob et al. (2014). After removing from the coagulation bath, the membranes were stored for at least 24 h before testing their fluxes and rejection properties. The numbers on the bars in Figure 4.1 represent the storage time for membranes in DI water. As seen from the results at the end of 47 days of storage in DI water, the PWP of the membrane (PSf:SPES blend ratio : 4) decreased from 103 L/m^2hbar to 49 L/m^2hbar. This was attributed to bacteria formation on the surface and it was concluded that during very long storage of membranes special precaution is needed to prevent bacteria formation.

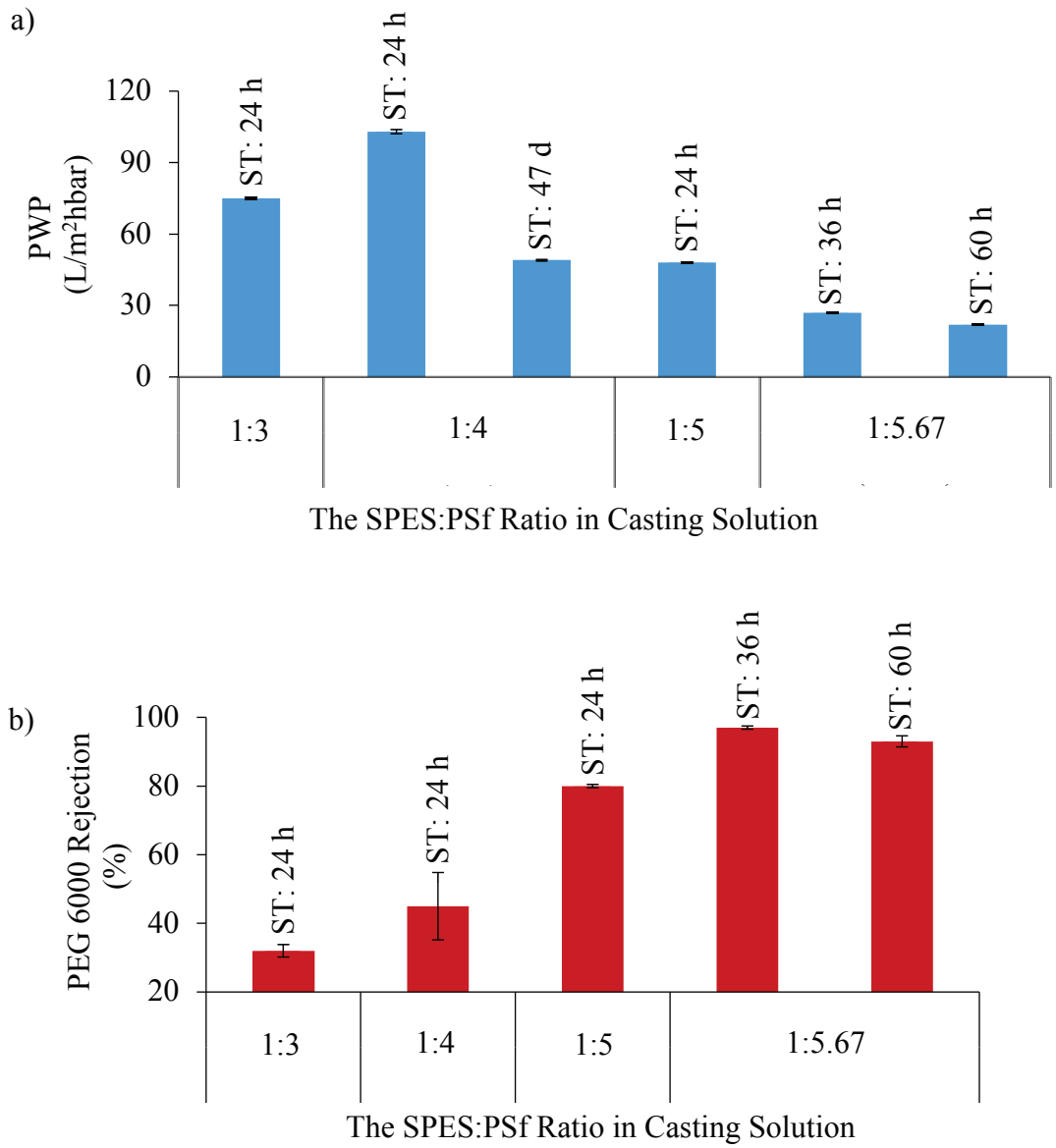

Figure 4.1. The effect of SPES:PSf ratio on a) PWP and b) PEG 6000 rejection of support membranes. **ST: Storage time for membranes in DI water. The support membrane cast with 25% polymer concentration; casting thickness: 250 μm; coagulation bath: DI water; immersion time: 10 min.; coagulation bath T: 4°C; storage T: 4°C.

The support membranes prepared from the PSf:SPES blend ratio of 4:1 and 5:1 were coated with PBC and the PEG 1000 rejection values of the resulting membranes were measured as 27 ± 0.39% and 56 ± 0.91%, respectively. These values indicated that the TFC membranes are not in NF category.

Table 4.2. The effect of SPES:PSf ratio in the casting solution on the performance of the PBC coated TFC membranes.

	SPES:PSf 1:4		SPES:PSf 1:5	
	Support	PBC coated	Support	PBC coated
PWP ($L/m^2.h.bar$)	103 ± 0.86	29 ± 0.38 28 ± 0.18	48 ± 0.22	14 ± 0.09 8 ± 0.03
PEG 6000 Rejection (%)	45 ± 9.8	96 ± 0.27	80 ± 0.47	100
PEG 1000 Rejection (%)	-	27 ± 0.39	-	56 ± 0.91

** Molecular weight of PBC: 25 kDa; concentration: 18 mg/mL; pH: 4.0; solution T: 25^{o}C; coating time: 24 h; washing time: 30 min.

The mechanical strength of the membranes cast on glass was really low thus, to improve their mechanical strength, it was decided to cast membranes on nonwoven fabrics. In the following section, the results for support membranes prepared on nonwoven polyester fabric were discussed.

4.2. Membrane Preparation with Polyester Nonwoven Fabric

The choice of nonwoven fabric is critical, it should have high porosity and connected pores to minimize mass transfer resistance, narrow pore size distribution and small pores on the surface to avoid penetration of polymer solution in the pores. In addition, the membrane should not detach from the nonwoven fabric. Four different types of nonwovens supplied from different companies (Grade 3329 (AHLSTROM), Novatexx 2484, Novatexx 2413, Novatexx 2471, 05TH-100 (HIROSE Paper Company)) were tested. Except sample 05TH-100, in other samples polymer solution penetrated into the fabric and a uniform membrane layer was not obtained on the surface. Therefore, the membranes were prepared with the polyester nonwoven supplied by HIROSE Paper Company.

4.2.1 Membranes Prepared From PSf:SPES Blend Ratio of 4:1

4.2.1.1. Effect of Casting Thickness

The 25% polymer solution was cast on the nonwoven fabric with 120 and 150 µm casting thicknesses. The PWP slightly increased while PEG 6000 rejection did not significantly change with the increased wet thickness. This was because at 120 µm casting thickness the solution partially penetrated into the pores leading to reduction in pore size of the nonwoven and a continuous layer on the fabric could not be achieved and defect formation was observed therefore the PEG 6000 rejection was very low. Similar result was reported by Boussu et al (2006). Based on this result, it was decided to continue casting the solution with 250 µm thickness.

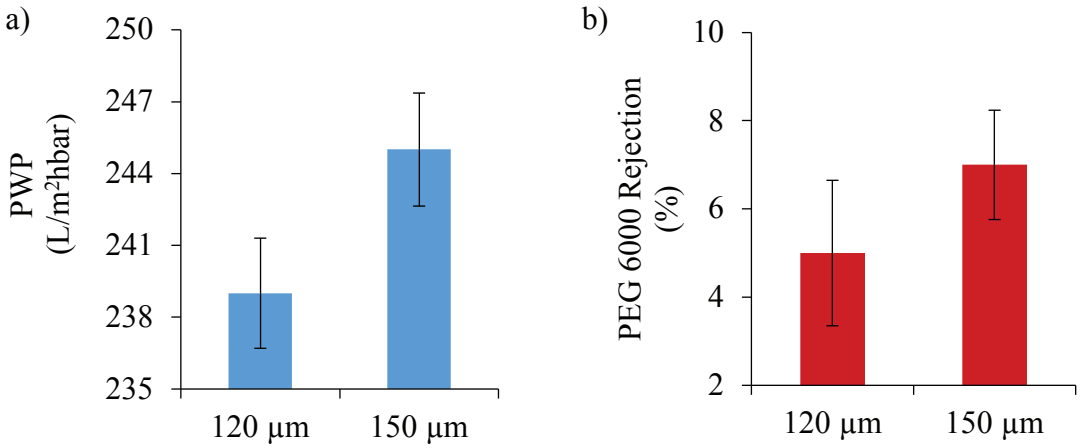

Figure 4.2. The effect of casting thickness on a) PWP and b) PEG 6000 rejection. **The support membrane was cast with 25% polymer concentration; coagulation bath: DI water; immersion time: 10 min.; coagulation bath T: 4ºC; storage T: 4ºC.

4.2.1.2 Effect of Coagulation Bath Composition

The results obtained from casting on the glass plate showed that the support membrane should have more than 50% PEG 6000 rejection to achieve NF membrane after PBC coating. In order to minimize the pore size of the membrane surface, the new strategies needed to be applied to prevent instantaneous phase inversion. Figure 4.3 shows that when instantaneous demixing occurs, the large macrovoids and fingerlike structure

are observed. On the contrary, delayed demixing forms spongy structure with smaller pores.

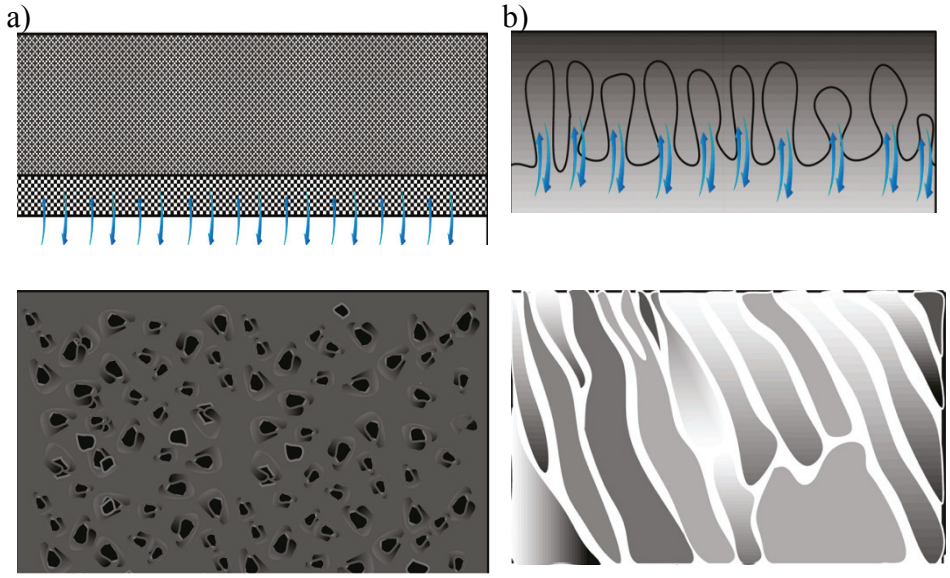

Figure 4.3. a) Delayed demixing and spongy like structure, b) Instantaneous demixing and fingerlike structure. (Source: Reprinted with permission from Mohsenpour et al., 2016)

Coagulation bath composition is one of the most important parameter to control the rate of demixing. The rate of exchange of solvent and components in coagulation bath can be reduced by either increasing the viscosity of coagulation bath or decreasing the surface tension of the bath. Anionic sodium dodecyl sulphate (SDS) (Mw:288.38) or nonionic TWEEN 80 (Mw:1310) was added into coagulation bath to increase the viscosity as well as to decrease the surface tension of the coagulation bath simultaneously. The membrane performances of prepared with these two surfactants were shown in Figure 4.4. The selection of concentrations of surfactants is crucial. Alsari et al. (2001) reported that smallest MWCO and pore size was obtained at 4^{o}C coagulation bath temperature and 1.2 mg/mL SDS concentration which is lower than the critical micelle concentration of SDS. Based on the findings reported in this study, the SDS and TWEEN 80 compositions in the coagulation bath were adjusted at 1.2 mg/mL SDS or 30x10^{-6} mol/L, respectively.

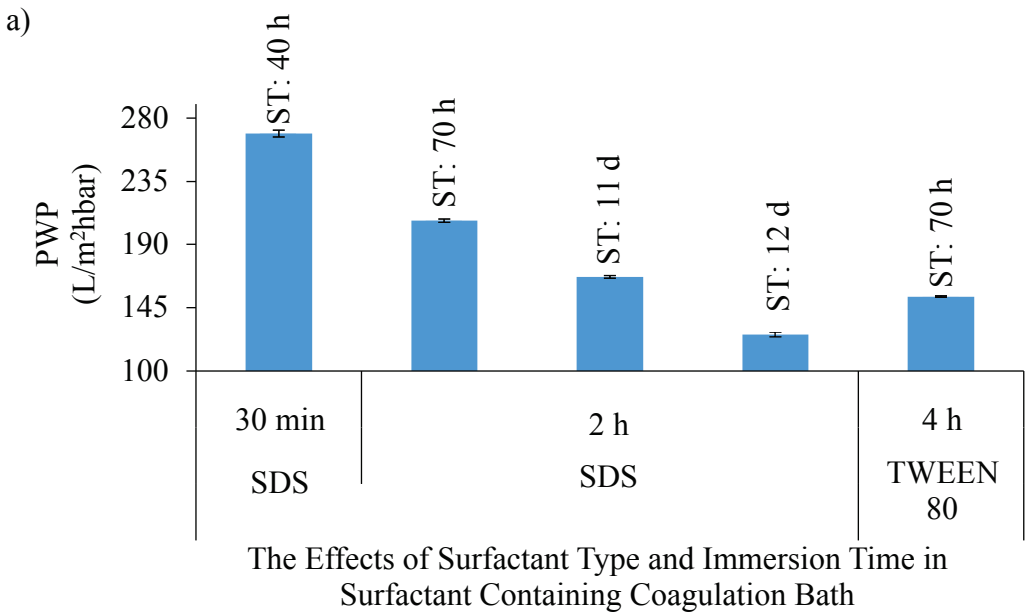

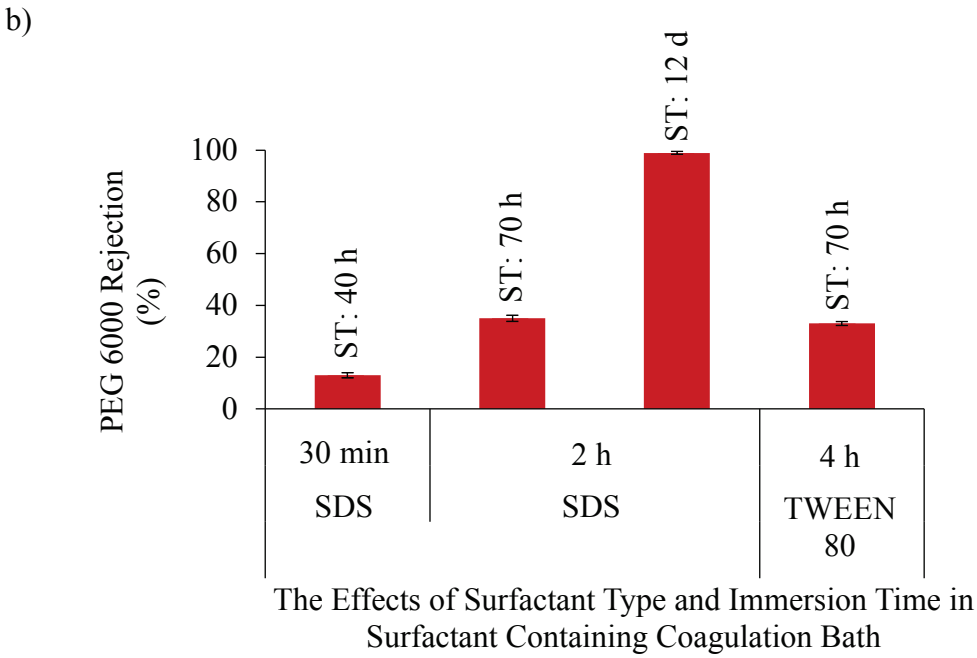

Figure 4.4. The effect of surfactant type on a) PWP and b) PEG 6000 rejection. ** ST: Storage time for membranes in DI water. The support membrane was cast with 25% polymer concentration; casting thickness: 250 μm; surfactant concentration in coagulation bath: 1.2 mg/mL SDS or $30x10^{-6}$ mol/L TWEEN 80; immersion time for SDS solution: 30 min or 2 h; immersion time for TWEEN 80: 4 h; coagulation bath T: 4°C; storage T: 4°C.

Membranes prepared by 30 min immersion in SDS containing coagulation bath had 270 L/m²hbar PWP and 13% PEG 6000 rejection. When immersion time increased to 2 h, PEG 6000 rejection increased from 13 % to 3 5%. At the end of 12 days of storage in DI water, the PEG 6000 rejection reached to 100 % while the PWP dropped to 126 L/m²hbar. Using TWEEN 80 in coagulation bath did not give better results when

compared to SDS in coagulation bath. At the end of 70 h of storage in DI water, PWP of the membranes immersed in SDS added coagulation bath was higher compared to the case when coagulation bath contained TWEEN 80 added coagulation bath while their PEG 6000 rejection values were similar. At 4^{o}C coagulation, at critical micelle concentration crystallization of SDS molecules were observed. Hammouda (2013) also reported that SDS molecules forms crystals below 10^{o}C. The presence of crystals affected the rate of phase separation negatively and increased the possibility of undesirable hole formation on the membrane surface. Based on this observation the concentration of SDS and coagulation bath temperature were fixed at 1.1 mg/mL and 15^{o}C, respectively.

4.1.2.3. Effect of Pre-evaporation

The combination of dry wet phase inversion has been used in controlling the membrane morphologies. In this combined process, first of all the casting solution is evaporated for a certain period of time and then immersed into the coagulation bath. During the evaporation step, top surface of the membrane becomes dense in polymer and dense skin layer formation is observed. By changing the evaporation time prior to immersion, the porosity and pore size, hence performance of the membrane can be adjusted (Arya, 2012). Figure 4.5 shows that 30 sec evaporation before coagulation significantly reduced the PWP of the support membrane below 20 L/m^2.h.bar. As seen from the results, storing membranes in DI water up to 15 days did not change its permeability which indicated that membrane structure is stable. When all the results were taken into account it was concluded that the support membranes prepared with PSf:SPES blending ratio of 4:1 had low PWPs. Consequently, it was decided to increase the content of more hydrophilic polymer SPES in the casting solution. In the following section, the results obtained with the membranes prepared from a PSf:SPES blending ratio of 3:1 were presented.

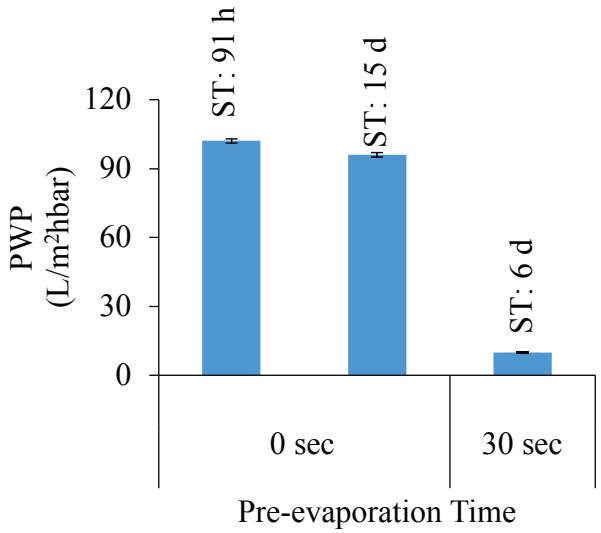

Figure 4.5. The effect of pre-evaporation step on PWP. ** ST: Storage time for membranes in DI water. The support membrane was cast with 25% polymer concentration; casting thickness: 250 μm; coagulation bath: 1.1 mg/mL SDS solution; immersion time for SDS solution:2 h; coagulation bath T: 15ºC; storage T: 4ºC.

4.2.2. Membranes Prepared with PSf:SPES Blending Ratio of 3:1

4.2.2.1. Effect of Solvent Type

When the SPES amount in the casting solution was increased, the solution did not appear completely transparent which indicated that NMP was not a very good solvent. The solubility parameters of solvents and polymers are used to choose the appropriate solvent. Simply, as the difference between the solubility parameters of solvent and polymer approaches to zero, $|\delta_P - \delta_s| \to 0$, the solvent power increases. NMP is a good solvent for PSf while DMAc is for SPES, therefore, it was decided to use a blend of these two solvents. Table 4.3 lists the solubility parameter difference between the PSf:SPES polymer blend and DMAc:NMP solvent blend. According to the results, the best solvent ratio for dissolving 1:3 SPES:PSf blend was found as 1:2 NMP:DMAc.

Table 4.3. The difference of solubility parameters of polymer and solvent.

	$(\delta_{polimer} - \delta_{solvent})^2$				
PSf:SPES	**DMAc:NMP**				
	0:1	**1:1**	**2:1**	**3:1**	**5:1**
1:0	4.48	4.29	4.37	4.43	4.51
3:1	4.30	3.83	3.82	3.85	3.89
4:1	4.33	3.91	3.92	3.96	4.01
0:1	4.71	3.44	3.09	2.95	2.82

Figure 4.6 shows that using DMAc:NMP mixture in the casting solution rather than NMP alone decreased the PWP of the support membrane. PEG 1000 rejection of the membranes prepared with pure NMP was 12% after 8 days of storage in DI water whereas it was 16 % at the end of 3 days of storage in DI water when the polymers were dissolved in NMP:DMAc mixture. It was decided to continue dissolving polymers in 1:2 NMP:DMAc solvent mixture due to higher PEG 1000 rejection and more homogeneous casting solution obtained with this solvent mixture.

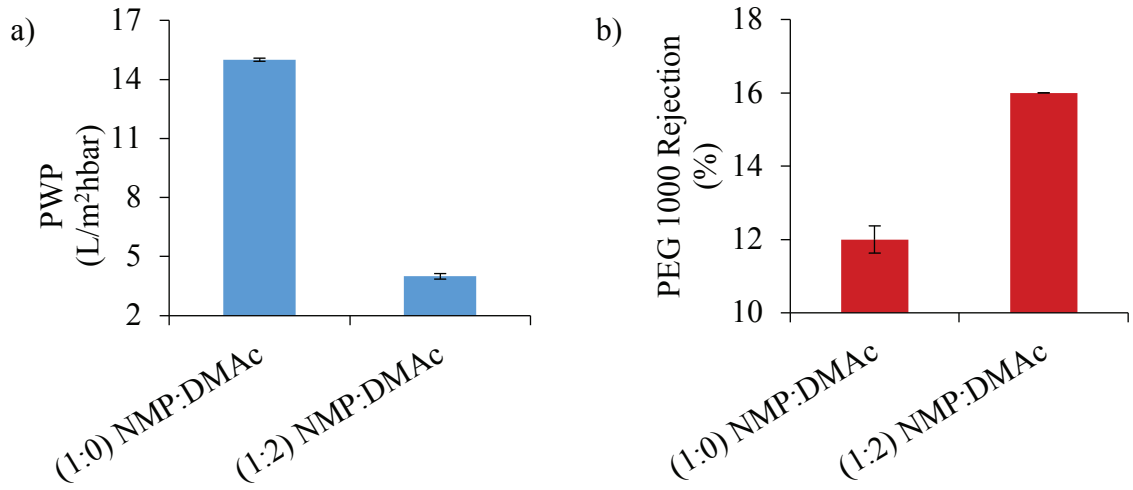

Figure 4.6. The effect of solvent type on a) PWP and b) PEG 1000 rejection. ** The support membrane cast with 25% polymer concentration; wet thickness: 250 µm; coagulation bath: 1.1 mg/mL SDS solution; immersion time for SDS solution: 2 h; coagulation bath T: 15°C; storage T: 4°C.

4.2.2.2. Effect of Casting Protocol

It was seen that during immersion in coagulation bath penetration of water from the back side of the nonwoven fabric caused 2-sided mass transfer leading to

instantaneous phase inversion and large pore size formation on the surface of the membrane. In order to prevent water penetration between nonwoven fabric and glass support, water resistant tapes were used. It was observed that the membranes prepared according to this protocol (Protocol 2) had lower PWP, but 3 times higher PEG 1000 rejection than the membranes prepared in the case of water infiltration between polyester and glass (Protocol 1). As can be seen from Figure 4.7, by allowing mass transfer only from top surface of the membrane, the PEG 1000 rejection increased from 16% to 50% while the PWP decreased by a factor of 2. In order to obtain small pores on the surface of support membrane, the precaution was taken in further studies to allow only one-sided mass transfer.

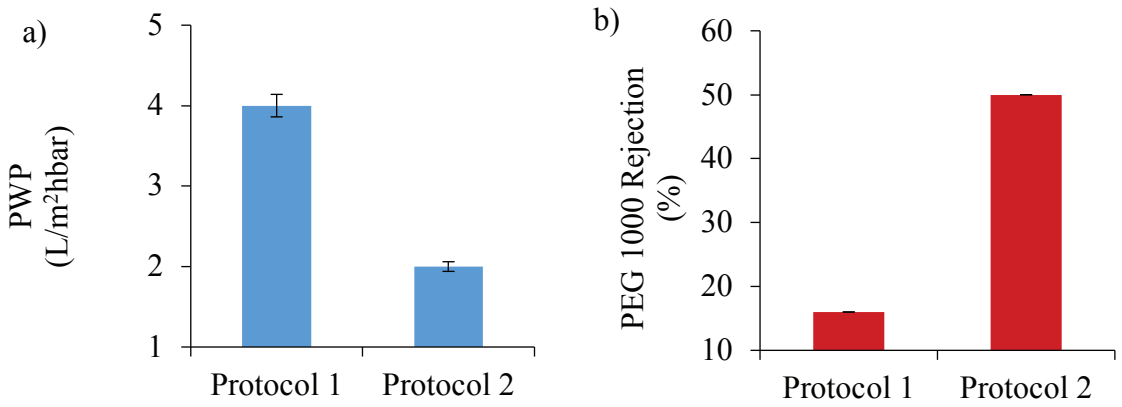

Figure 4.7. The effect of casting protocol on a) PWP and b) PEG 1000 rejection. ** The support membrane was cast with 25% polymer concentration; wet thickness: 250 µm; coagulation bath: 1.1 mg/mL SDS solution; immersion time for SDS solution: 2 h; coagulation bath T: 15°C; storage T: 4°C.

Membranes were prepared by pre-evaporation for 15 and 30 sec with the new protocol. As the evaporation time increased, the PWP of the membranes dramatically decreased while PEG 1000 rejection increased (Figure 4.8). When the membranes prepared by pre-evaporation for 15 sec were coated with PBC, PWP decreased to 1 L/m²hbar and PEG 1000 rejection increased to 43%. It was seen that the TFC membrane prepared is not in NF category. This was directly attributed to insufficient structural features of the support membrane.

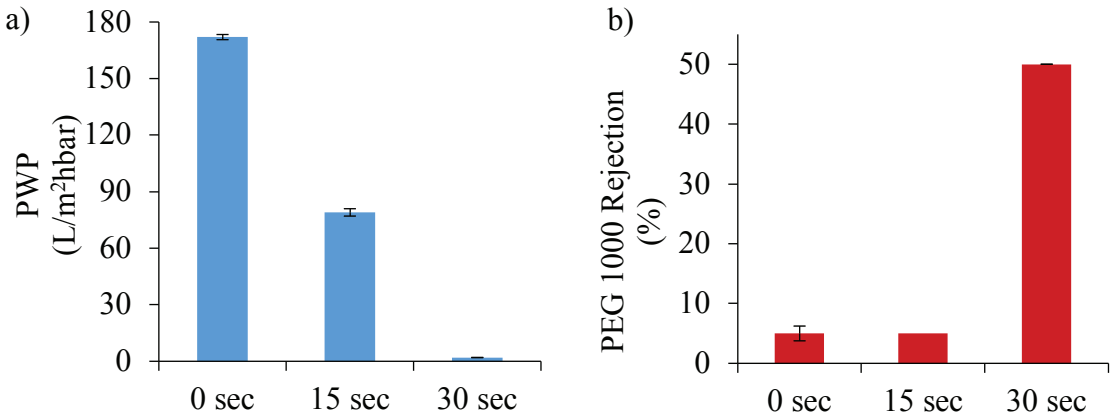

Figure 4.8. The effect of evaporation time with protocol 2 on a) PWP and b) PEG 1000 rejection. ** The support membrane cast with 25% polymer concentration; wet thickness: 250 μm; coagulation bath: 1.1 mg/mL SDS solution; immersion time for SDS solution: 2 h; coagulation bath T: 15°C; storage T: 4°C.

4.2.2.3. Modification of Membranes Prepared on Nonwoven Support with Polyelectrolytes

Despite the fact that many parameters during membrane preparation have been changed, desired PWP and surface pore sizes have not been achieved in prepared membranes. In the case of support membranes which are not sufficiently small in surface pore size, the composite membrane which rejects 80-90% of PEG 1000 could not be obtained. To reduce the surface pore size of the support membrane, it was decided to coat the negatively charged support membrane first with a cationic polyelectrolyte PEI and then with an anionic polyelectrolyte ALG. As can be seen from Figure 4.9, the PWP of the uncoated support membrane decreased from 31 L/m^{2}hbar to 6 L/m^{2}hbar after coating with PEI and ALG, while the PEG 1000 rejection increased from 5% to 56%. Both PWP and rejection values were found unacceptably low.

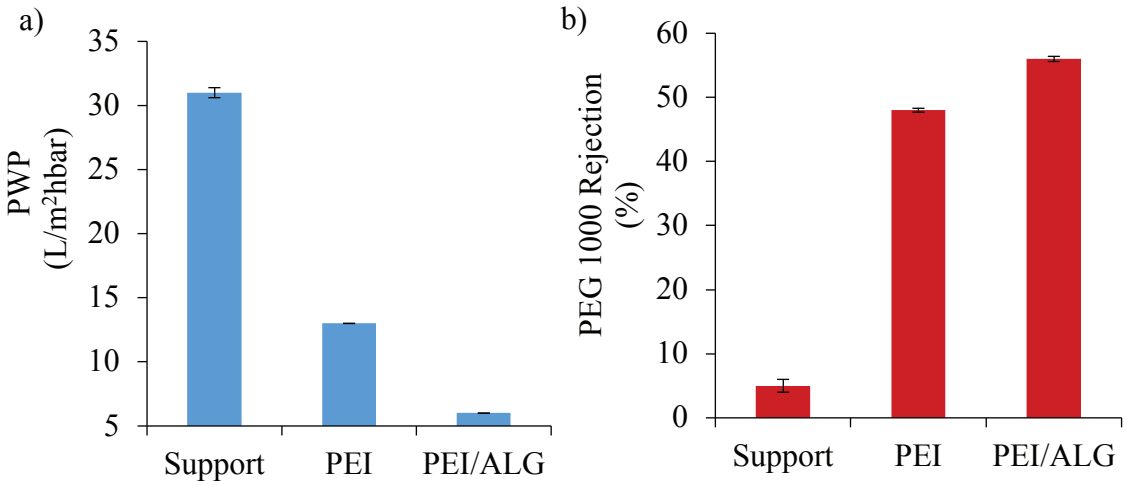

Figure 4.9. Polyelectrolyte coated membrane a) PWP and b) PEG 1000 rejection. ** The support membrane was cast with 25% polymer concentration; wet thickness: 250 µm; coagulation bath: 1.1 mg/mL SDS solution; immersion time for SDS solution: 2 h; coagulation bath T: 15°C; storage T: 4°C; evaporation time: 15 sec.

As a next strategy, instead of SDS, PEI (750 kDa) was added into the coagulation bath. During coagulation, the PEI diffused from the coagulation bath to the polymer solution and electrostatically attached to the negatively charged SPES and the unbounded PEI was removed from the membrane during storage in water. The support was then modified with alginate under dynamic conditions to cover all the pores before attaching PBC. The PEG 1000 rejection of the ALG modified support was determined as 69% (Table 4.4), on the other hand, the results were found not reproducible when the samples from different part of the membrane were tested. This was attributed to the presence of PEI which was not easily removed from the membrane due to its high molecular weight.

Table 4.4. The effects of uncoated and coated membranes on PWP and selectivity.

	Uncoated Membrane		ALG coated membrane	
	2 days	3 days	2 days	3 days
PWP (L/m^2hbar)	13 ± 0.34 23 ± 0.26	37 ± 0.18	- 7	11 ± 0.07
PEG1000 Rejection (%)	81 ± 0.62 -	24	- -	69 ± 0.43

** The support membrane cast with 25% polymer concentration; ratio of PSf:SPES: 3; wet thickness: 250 µm; coagulation bath: 0.5 wt% PEI soln.; Mw of PEI: 750 kDa; immersion time; 8 h; coagulation bath T: 25°C.

In the next trial, the membranes were prepared under the same conditions but using 25 kDa PEI instead of 750 kDa in the coagulation bath and this approach allowed obtaining reproducible results. As can be seen from Figure 4.10, the PWP of the support membrane decreased from 40 L/m^{2}hbar to 15 L/m^{2}hbar when PBC was coated, while the PEG 1000 rejection increased from 24% to 87%. The ultimate goal in the thesis was to achieve stimuli-responsive TFC NF membrane with a PWP not less than 10 L/m^{2}hbar and MWCO value of at least 1 kDa (corresponding to 90% PEG 1000 rejection). The results in Figure 4.10 shows that this objective has been ultimately achieved.

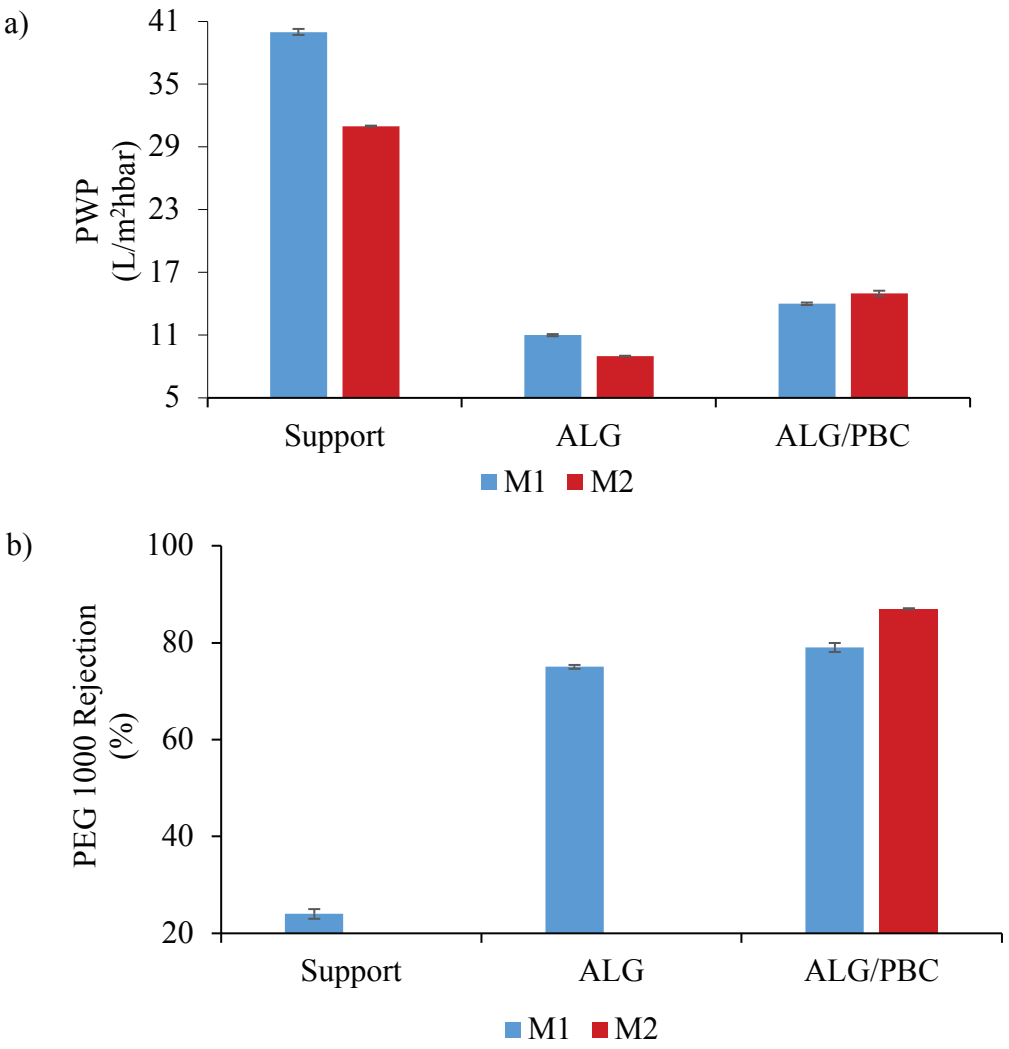

Figure 4.10. Uncoated and ALG/PBC coated membrane a) PWP and b) PEG 1000 rejection. **The support membrane was cast with 25% polymer concentration; ratio of PSf:SPES: 3; wet thickness: 250 µm; coagulation bath: 0.5 wt% PEI solution.; Mw of PEI: 25 kDa; immersion time; 8 h; coagulation bath T: 25^{o}C; M1 and M2 are the pieces that are cut from different parts.

4.3. Adsorption Kinetics of PBC

Previous studies have shown that the entire tertiary amine groups (pKa = 7.6) in the PBC at pH = 3.0 - 4.0 carry the maximum cationic charge as a proton (Determan et al., 2005) and critical micelle concentration at 25°C is 20 mg/mL (Determan et al., 2006). Based on these results, adsorption experiments were carried out at 25°C by adjusting the pH of PBC solutions (prepared from 15, 20 and 25 kDa copolymers) to 4.0 and the concentration to 6, 8, 12 and 18 mg/mL. It was expected that protonated cationic tertiary amine groups of PBC are electrostatically attached to the carboxyl groups of the ALG-coated support. Figures 4.11 through 4.13 show the change in the amount of copolymer grafted to the surface as a function of time.

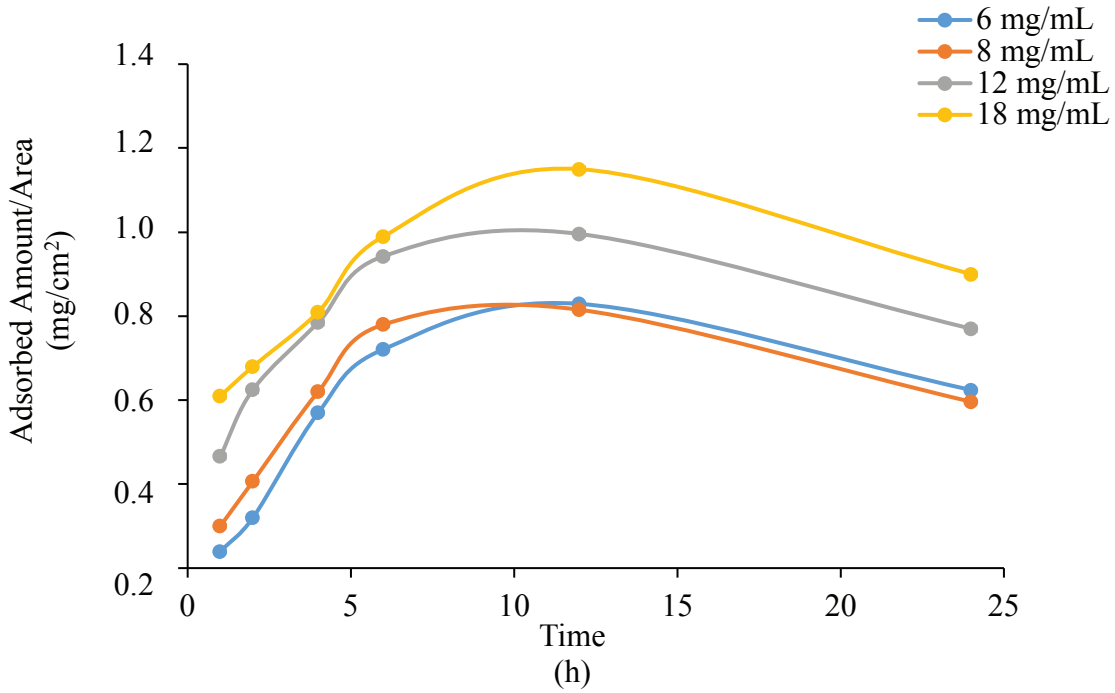

Figure 4.11. The change of amount of 15 kDa PBC adsorbed on the membrane with respect to time.

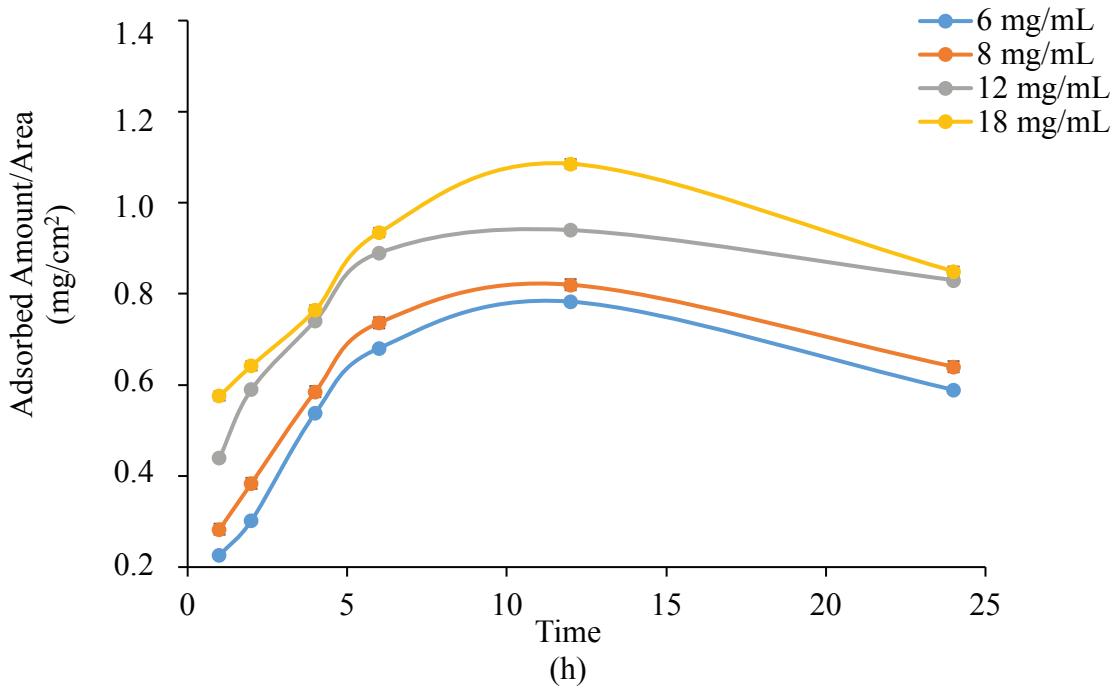

Figure 4.12. The change of amount of 20 kDa PBC adsorbed on the membrane with respect to time.

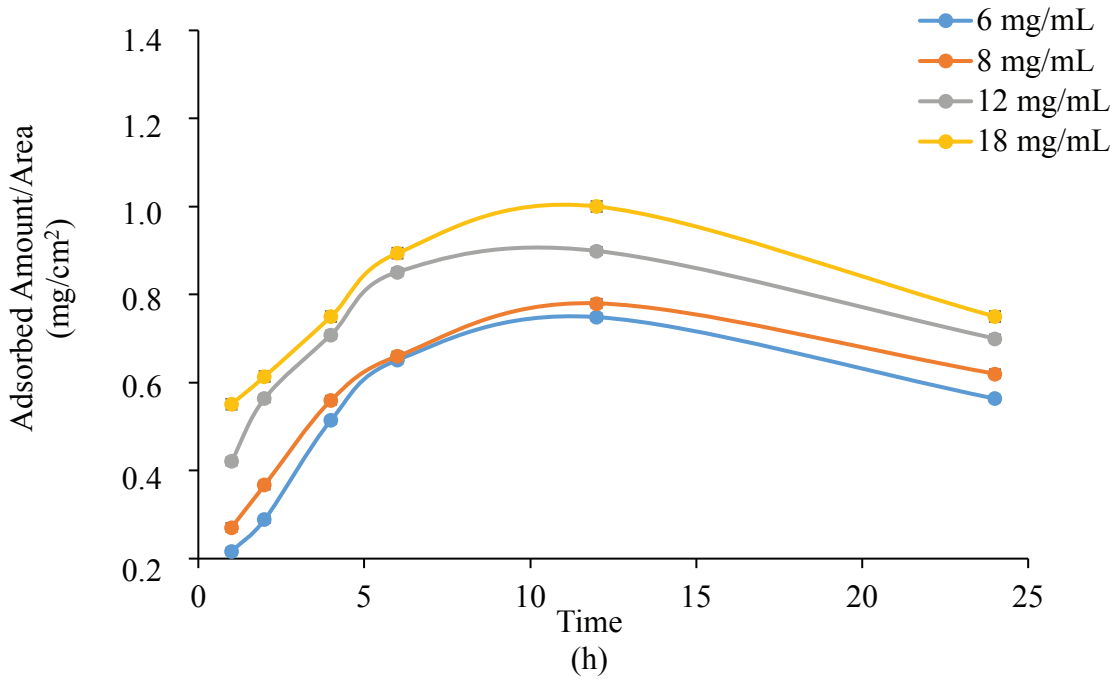

Figure 4.13. The change of amount of 25 kDa PBC adsorbed on the membrane with respect to time.

Regardless of the molecular weight of the copolymer, the grafted amount reached a maximum at the end of 12 h then a decrease was recorded. This is due to segment-segment repulsion between polymer chains over the time. Figure 4.14 schematically shows the steps during adsorption of the copolymer.

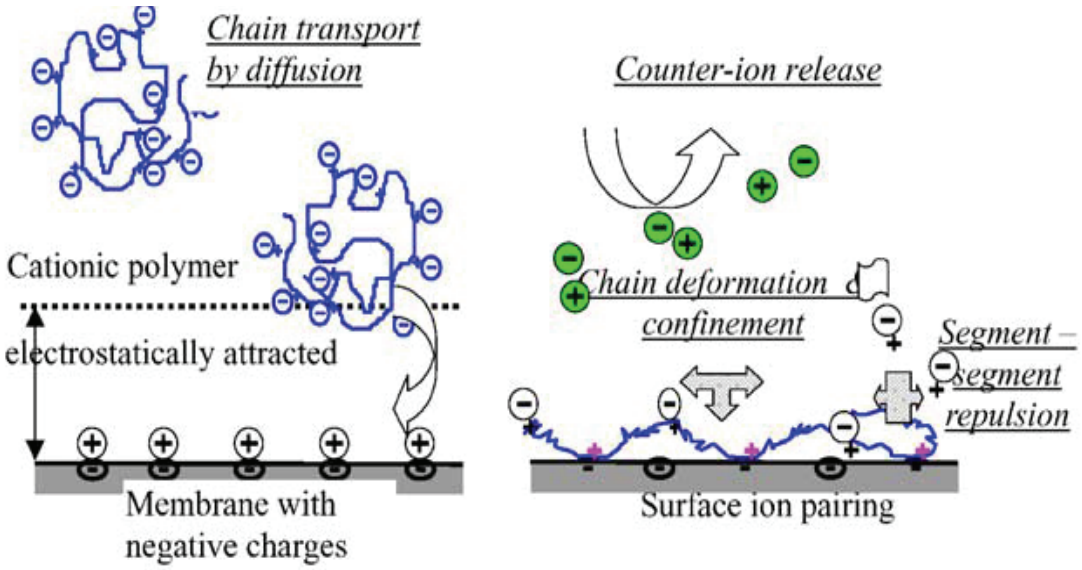

Figure 4.14. The affinity of the cationically charged group-carrying copolymer to the negatively charged membrane surface. (Source: Reprinted with permission from Nguyen et al., 2004)

Initially, when the support surface is empty, the copolymer adsorbs rapidly to the surface. Once the surface is completely covered by the copolymer, the free copolymer tries to adsorb to those that are attached. However, due to repulsion between copolymer chains, the conformational change occurs leading to desorption of some of the attached chains. Decrease in the amount of adsorbed block copolymer over time has also been reported by Zhao et al. (2005). According to the results, maximum adsorbed amount slightly decreased with the increase in the molecular weight of the copolymer. This observation is consistent with the theory developed by Dan and Tirrell (1993). According to this theory;

$$A\alpha \frac{1}{(N_B)^{0.2}} \tag{4.1}$$

Adsorbed amount (A) is inversely proportional to block length. Using this theory, the ratio of amount of 25 kDa copolymer adsorbed to the 15 kDa copolymer was estimated as 0.87. This value is consistent with experimental measurement where the amount of copolymer adsorbed decreased from 1.15 to 1 mg/cm^2 when the molecular weight of the copolymer changed from 15 to 25 kDa.

4.4. Surface and Morphological Properties and Water Permeabilities of Uncoated and TFC membranes

SEM was used to study the effect of modification on the appearance and structure of the membranes. Figures 4.15 through 4.18 show images obtained by SEM of support and composite membranes prepared by coating support with PBC of ~ 15 kDa, ~ 20 kDa, ~ 25 kDa molecular weight. These cross-section structures are typical for polymer membranes obtained by nonsolvent induced phase separation (NIPS). In the previous studies, it has been shown both theoretically and experimentally that the formation of pores in the resultant finger-like structure indicates instantaneous phase separation (Guillen et al. 2011). Dense skin layer was obtained on the top and beneath this layer, larger voids were observed. This structure is called finger like sublayer, developed during the immersion and final film formation in the bath. Although both support and coated membranes have finger like sublayer structure, we have observed a changed in the top dense skin layer thicknesses of these membranes (Table 4.5). Qualitatively, the percentage of dense skin layer for the support was measured as 0.35% of the total thickness. For the TFC membrane, the percentage of dense skin layer increased from 0.35% to 0.63% which confirmed the presence of the coating on the support layer.

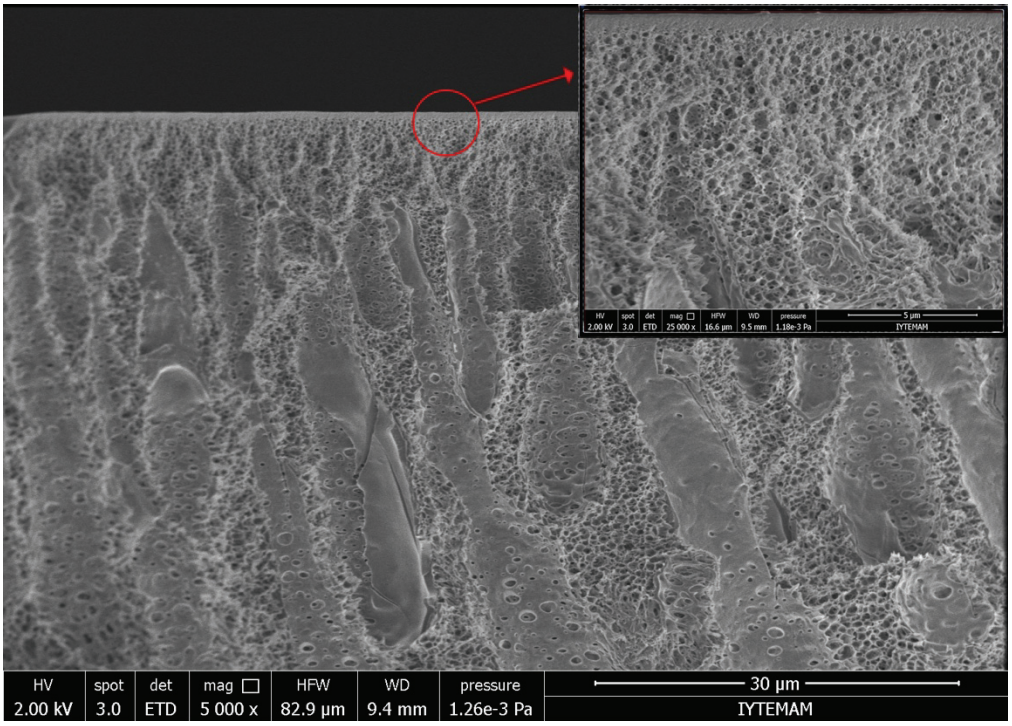

Figure 4.15. SEM images of cross-section of support membrane. Magnification x5000 and x25000.

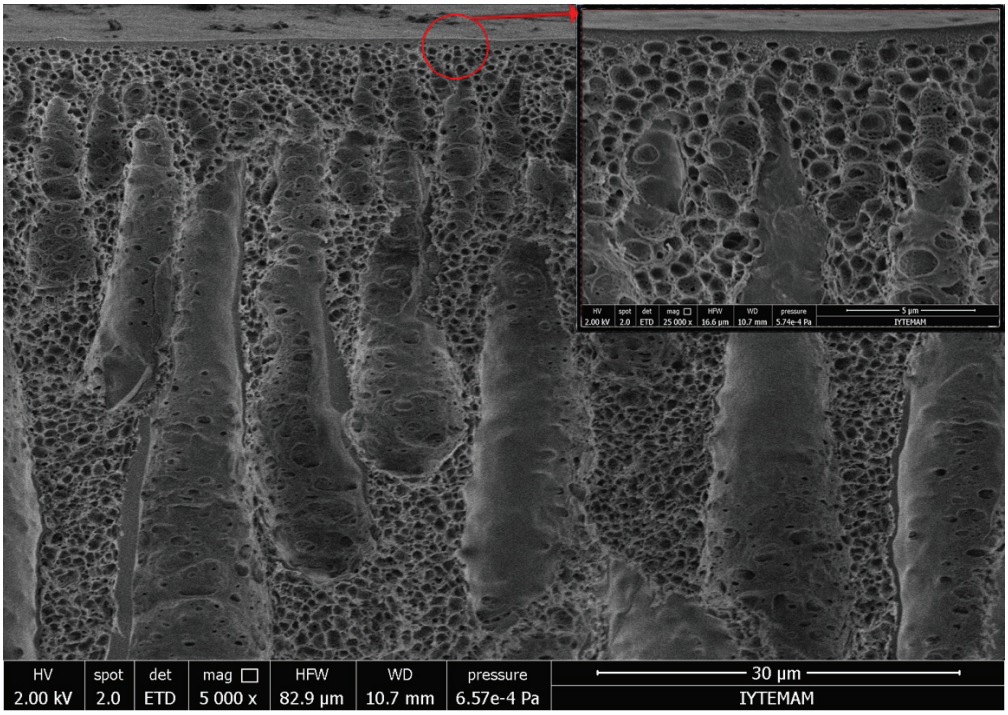

Figure 4.16. SEM images of cross-section of 15 kDa PBC coated membrane. Magnification x5000 and x25000.

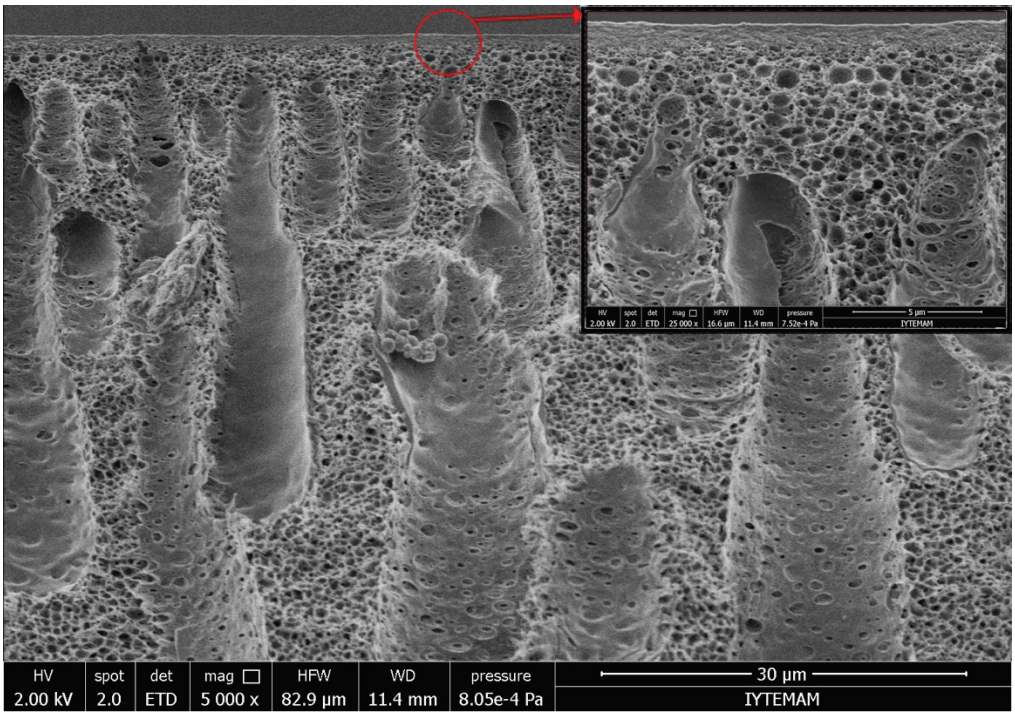

Figure 4.17. SEM images of cross-section of 20 kDa PBC coated membrane. Magnification x5000 and x25000.

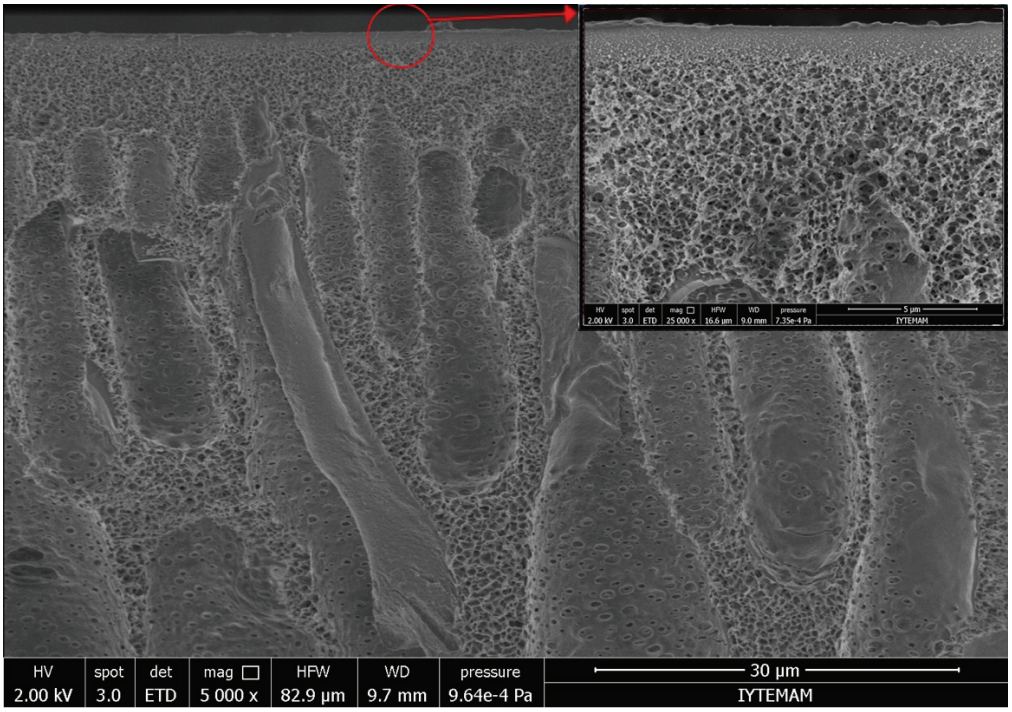

Figure 4.18. SEM images of cross-section of 25 kDa PBC coated membrane. Magnification x5000 and x25000.

Table 4.5. Dense skin layer thicknesses of support and TFC membranes

Membrane Code	**Dense Skin Layer Thickness (µm)**	**Percentage of Dense Skin Layer Thickness (%)**
Support membrane	0.58 ±0.013	0.35
TFC (15 kDa)	0.55 ±0.167	0.39
TFC (20 kDa)	0.91 ±0.050	0.56
TFC (25 kDa)	1.00 ±0.003	0.63

AFM was used to study the effect of coating on the membrane surface morphology. Figure 4.19 gives images of the surface roughness of control and TFC membranes. Corresponding root mean square (RMS) values were listed in Table 4.6. The coating of the support membrane with ALG reduced the surface roughness by 56%. However, no significant difference was observed between ALG and PBC coated membranes. This is because PBC forms a very thin layer on the surface and the properties of the ALG-coated membrane have been observed predominantly in roughness measurements.

a)

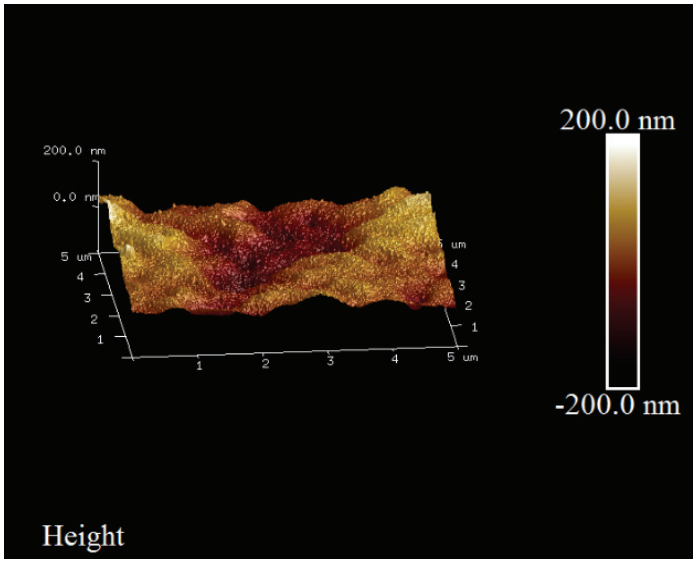

b)

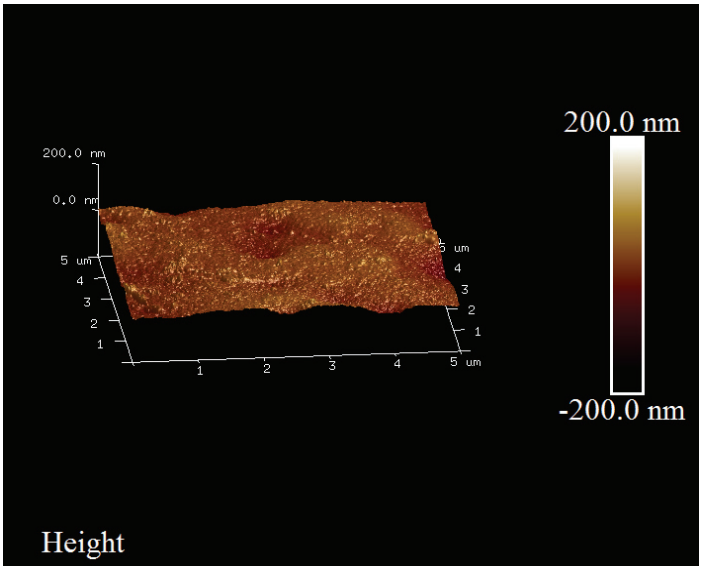

c)

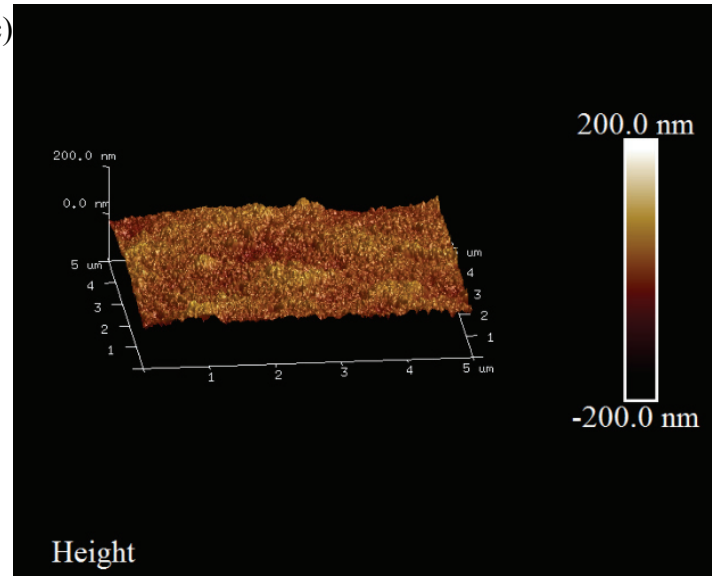

Figure 4.19. 3D AFM images of a) Suppport membrane, b) ALG coated, c) ALG/15 kDa PBC coated membrane, d) ALG/20 kDa PBC coated membrane, e) ALG/25 kDa PBC coated membrane.

d)

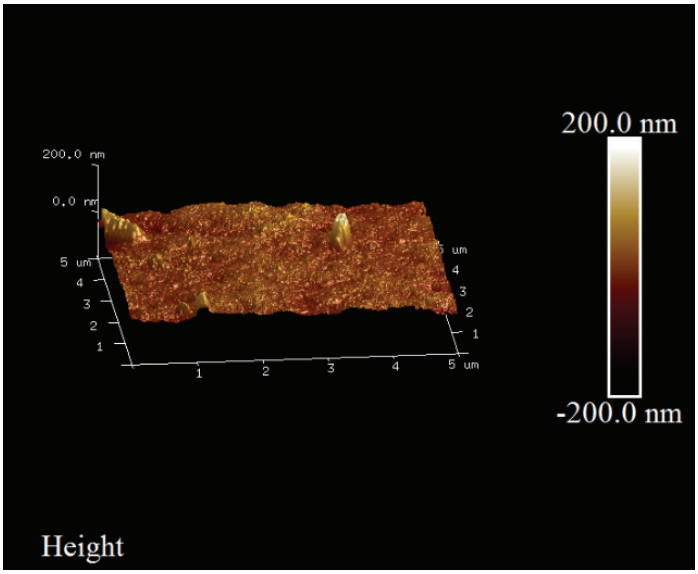

e)

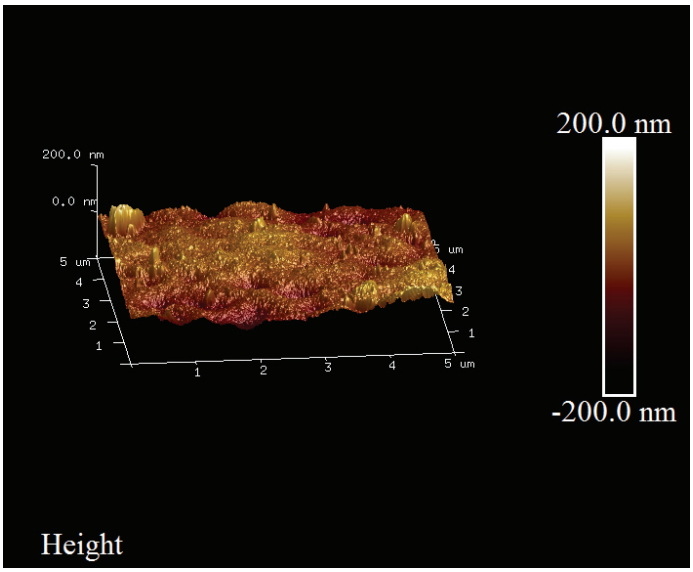

Figure 4.19. (cont.)

Table 4.6. Roughness results of support membrane and TFC membranes.

Membrane Code	RMS (nm)
Support membrane	24.8 ±1.16
ALG	10.8 ±1.04
ALG/15kDa PBC	9.52 ±0.57
ALG/20kDa PBC	9.27 ±1.29
ALG/25kDa PBC	9.79 ±0.37

Table 4.7. Contact angle values of support membrane and TFC membranes.

Membrane Code	Contact Angle Measurements			
	T: 4◦C pH: 7.6	T: 25◦C pH: 7.6	pH: 4 T: 25◦C	pH: 8.5 T: 25◦C
Support	65.3 ±1.9	66.4 ±1.8	72.1 ±0.9	67.4 ±1.0
TFC (ALG)	65.2 ±1.4	68.0 ±1.7	61.0 ±0.9	63.4 ±1.4
TFC (ALG/15 kDa PBC)	62.4 ±1.4	71.0 ±1.5	69.2 ±1.4	61.7 ±0.9
TFC (ALG/20 kDa PBC)	51.9 ±1.4	65.6 ±1.6	66.7 ±2.2	60.9 ±1.0
TFC (ALG/25 kDa PBC)	51.2 ±1.6	68.7 ±1.8	69.8 ±2.1	61.7 ±1.1

Table 4.7 lists the contact angles measured at the pH=pKa=7.6, pH < and pH>pKa and at T=4ºC < LCST (8ºC) and T=25ºC > LCST of the copolymer. It is seen that the coating resulted in decrease in the contact angle of the support membrane which indicated the improvement of its hydrophilic character. The hydrophilic/hydrophobic character of the membranes changed with pH and temperature. When chains are in stretched conformation at T=4ºC <LCST, the TFC membrane displayed more hydrophilic character compared to the case at T=25ºC. The effect of temperature responsiveness on the hydrophilic character of the TFC membrane was found higher than that of pH responsiveness of the chains. This is because pH responsiveness of the TFC membrane is caused not only by the PDEAEM end blocks of the copolymer but also by the ALG and PEI in the structure. On the other hand, the only temperature responsive group is the Pluronic F127 in the middle block of the copolymer.

Figures 4.20 and 4.21 show the XPS general survey spectrum of support and 25 kDa PBC coated membranes. The only different element in the PBC is bromide, however, it was not detected in the general survey since it is present in a small fraction. All other elements including, C, N, O and S were found on the support and coated membranes, but their quantities were different. As seen from the results in Table 4.8, sulfur (S1s) was observed only on the support membrane and the % of O and N elements were found higher in the TFC membrane. The deconvolution of C1s peak for both support and TFC membranes is shown in Figures 4.23 and 4.24. C-Br and O-C=O groups exist only in the PBC. The C-Br peak was not considered as a fingerprint since it overlaps with the C-C peak. It was seen that O-C = O (Binding energy: ~288.5 eV) appears only in the XPS spectra of the TFC membrane taken at 5º angle. These results proved the presence of the PBC on the support membrane.

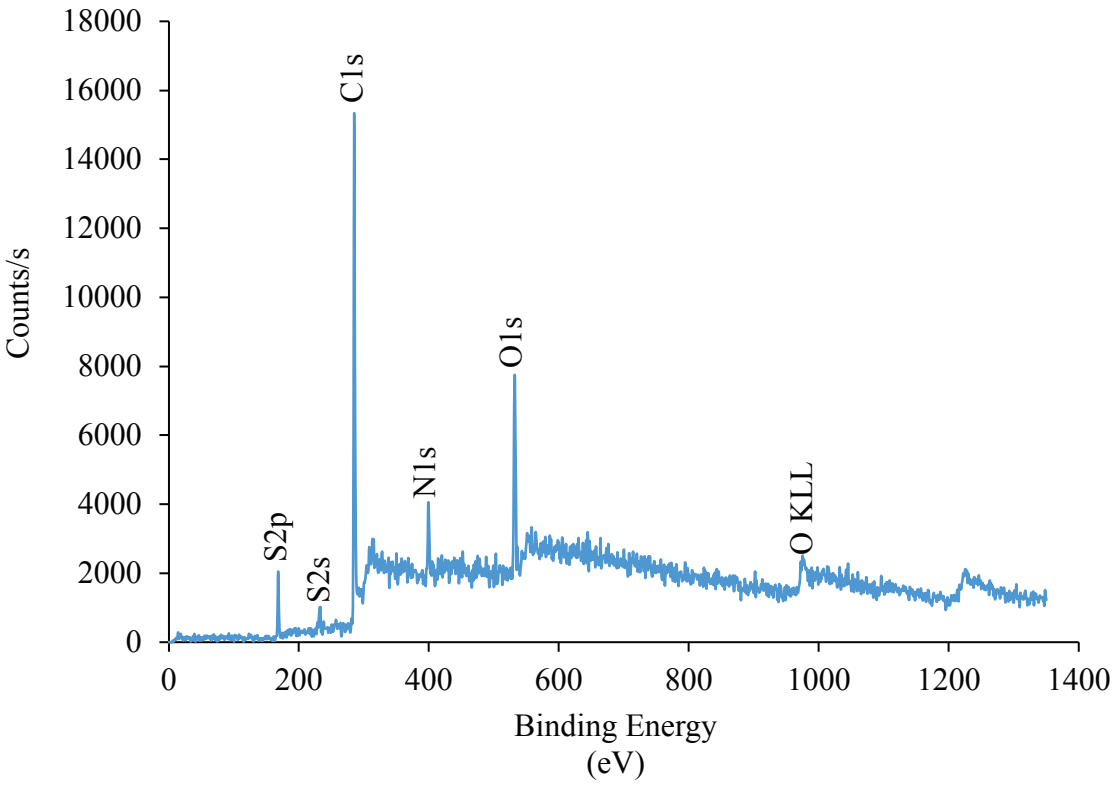

Figure 4.20. XPS spectrum of support membrane. Scanning angle 45◦.

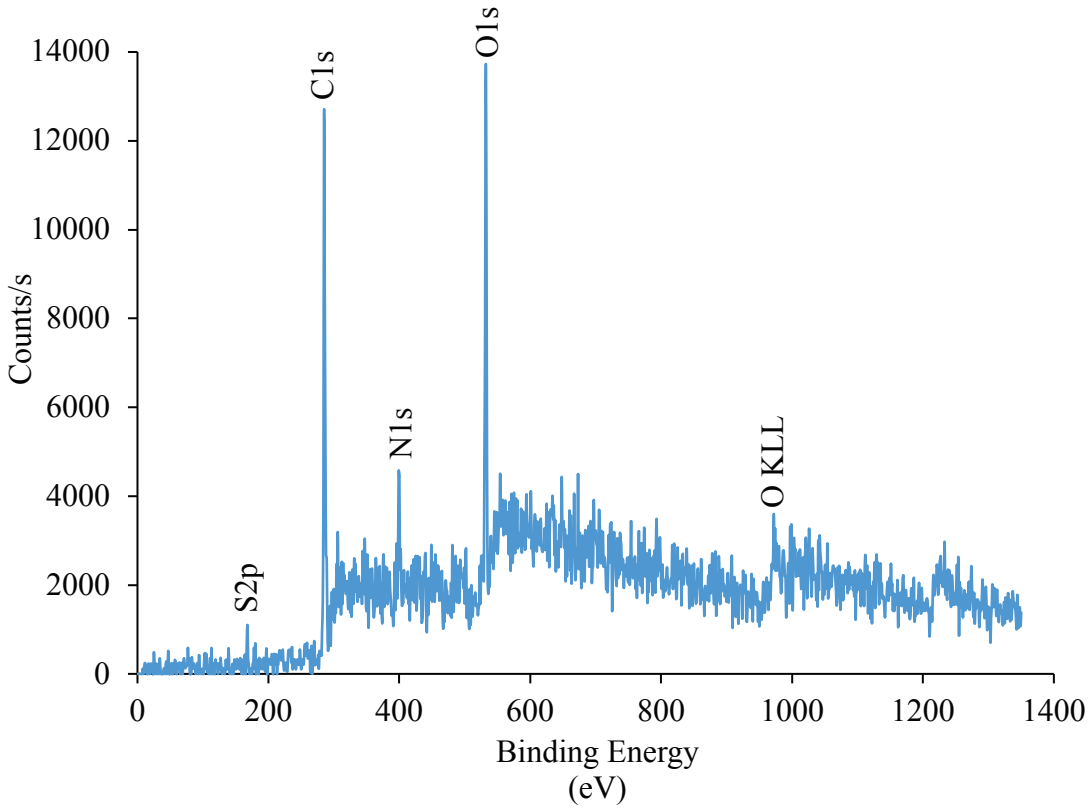

Figure 4.21. XPS spectrum of 25kDa PBC coated membrane. Scanning angle 45◦.

XPS data was also used to determine the conformation of PBC on the surface. Figure 4.22 shows three possible conformation of the copolymer when grafted on the support. The conformation is determined by the concentration of the PBC, the temperature and pH of the copolymer solution as well as coating time. As can be seen from Figure 4.22, it is expected that the PBC under its critical micelle formation concentration will be in the form of brush or loop conformation and in micelle form above this concentration (Lin and Alexandridis, 2002).

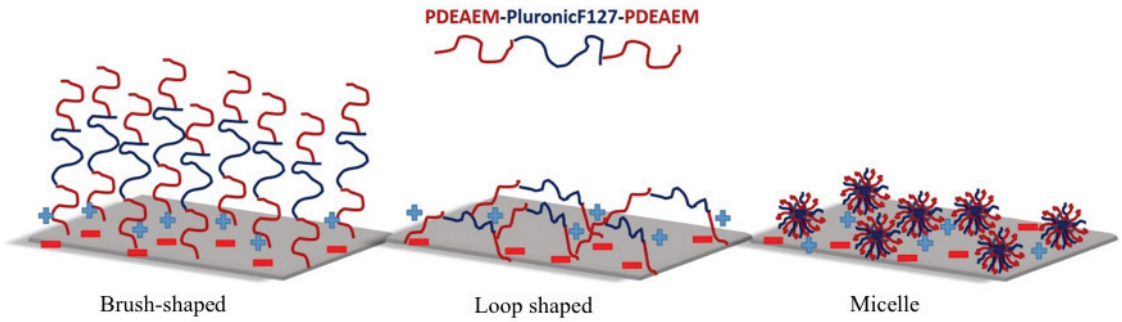

Figure 4.22. Conformation of PBC on membrane surface.
(Source: Drawn on the basis of Liu and Urban, 2010; Lee et al., 2010)

Table 4.9 lists the % of O-C = O group calculated from the spectra taken at 5° and 10°. Amount of O-C=O group increased with the increased scanning angle. This is because the block copolymer has PDEAEM blocks in the end groups and O-C=O group exists in these end blocks. With the increased scanning angle, the X-ray beam penetrates deeper into the membrane. At 5° O-C=O group in the outermost PDEAEM block was determined while at 10° both PDEAEM blocks were reached and both O-C=O groups were determined. This result proved that PBC has a brush-like configuration on the support surface.

Table 4.8. Atomic percentage values of support membrane and TFC membranes.
(Scanning angle: 45°)

	Atomic (%)			
	C1s	**N1s**	**O1s**	**S1s**
Support Membrane	34.87	5.02	7.77	2.17
25 kDa Coated Membrane	32.75	6.52	11.62	-

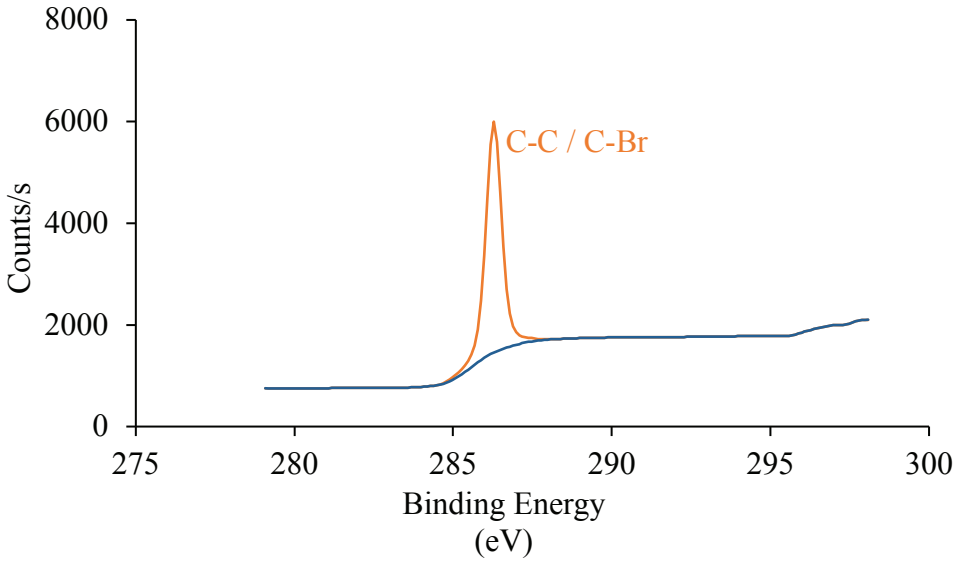

Figure 4.23. Support membrane with 5◦ scanning angle.

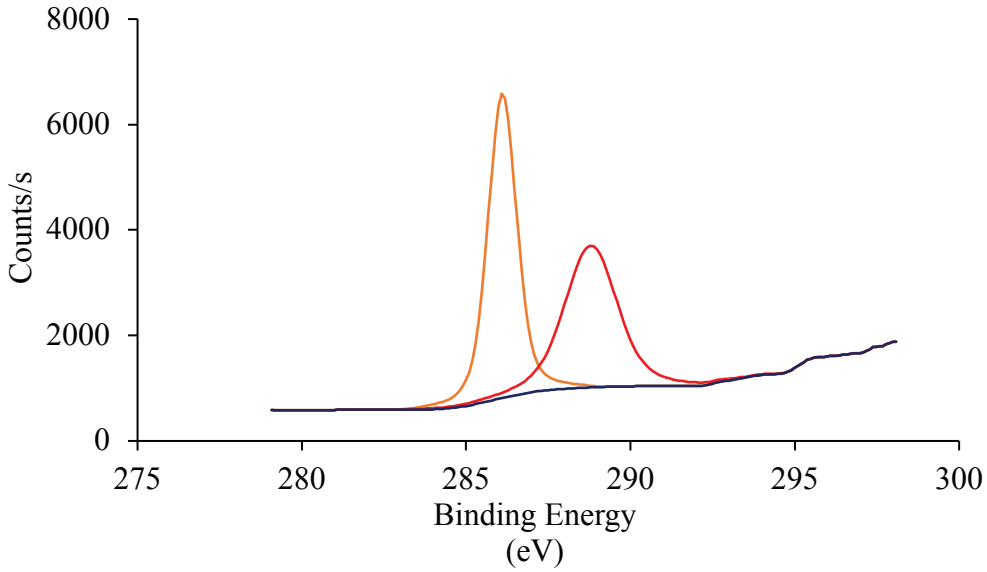

Figure 4.24. 25 kDa PBC coated TFC membrane with 5◦ scanning angle.

Table 4.9. Counts/s and atomic percentages of support membrane and TFC membranes.

	O-C=O	
Angle (°)	**Counts/s**	**Atomic %**
5	3700.85	3.7
10	4023.89	3.83

All the characterization results including the total thickness, dense skin layer thickness, surface roughness of the membranes, contact angle measurement and XPS

analysis proved that the PBC was successfully deposited on the surface of the support membrane.

Figure 4.25 demonstrates that the PWP of the support membrane decreased from 26.8 to 15 L/m^2.h.bar in the case of 15 kDa PBC. The molecular weight of the PBC had a slight influence on the permeability of the membrane. Combining PWP and contact angle measurements, the 25 kDa PBC was chosen for further studies since the TFC membrane prepared with this copolymer sample displayed the highest responsiveness. It is anticipated that the 25 kDa TFC membrane should provide higher rejection properties and mechanical properties than the 15 and 20 kDa TFC membranes. Tomer et al. (2009) examined the influence of chain length of the stimuli responsive polymers on the flux and rejection of the membranes. They studied temperature responsive PNIPAAm which was grafted onto the membrane by using ATRP method. They reported that increasing the polymerization time, hence, the chain length increased the thickness of dense polymer nanolayer and lowered flux but provided high rejection of the solutes.

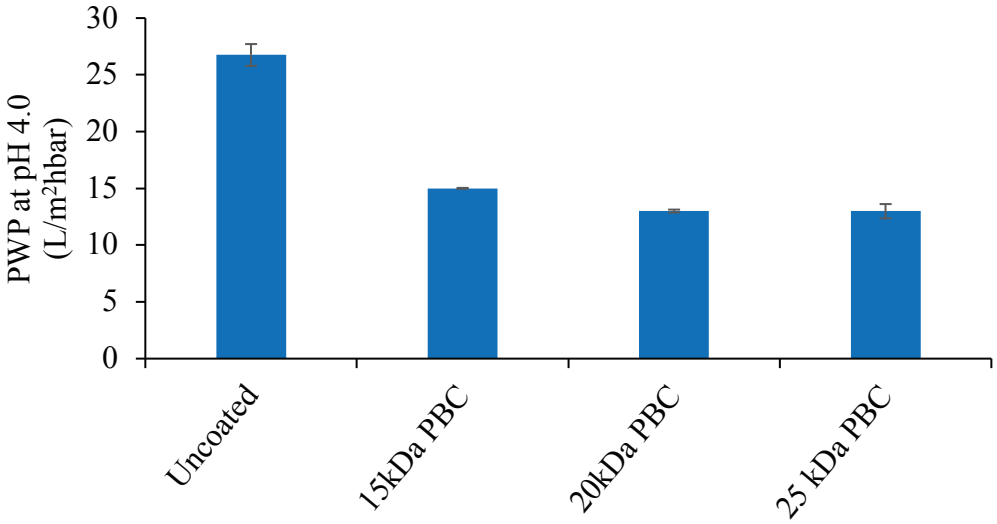

Figure 4.25. PWP measurements of support and PBC coated membranes with different molecular weights.

In the following section, the influences of pH and temperature of feed solution on the rejection of PEG 1000, pore size and molecular weight cutoff value of the membranes prepared from 25 kDa PBC were investigated.

4.5. The Effects of Solution pH and Temperature on the PWP and Rejection Properties of the Membranes

Figure 4.26 shows the change in the PWP and PEG 1000 rejection of the membranes with the pH of feed solution. The lowest rejection was observed at pH 4 and the highest at pH 8.5. The PWP increased from 13.0 ±0.63 to 15.9 ±0.06 L/m^2.h.bar upon changing the pH from 4.0 to 8.5. This occurs due to enhanced hydrophilic character of the membrane. As seen from the results in Table 4.7, the contact angle decreased almost 10 degrees as pH was raised from 4 to 8.5. At pH 8.5 adjusted with NaOH, OH molecules make hydrogen bonding with amine groups in PDEAEM leading to more hydrophilic surface than at pH 4. Another reason for the increased flux with pH is the switch between swollen and collapsed conformation of the PBC chains. The pKa of PBC in the selective layer of the TFC membrane was previously determined as 7.6 (Determan et al., 2005). At pH 4.0 below the pKa value, amine groups on the PDEAEM chains become deprotonated hence repel each other leading to more expanded structure and reduction in flux while at pH 8.5 the chains become uncharged and adopt a collapsed conformation. On the other hand, the results have shown that the change in the conformation of the chains as a result of pH stimulus response is modest for both the PWP and PEG 1000 rejection.

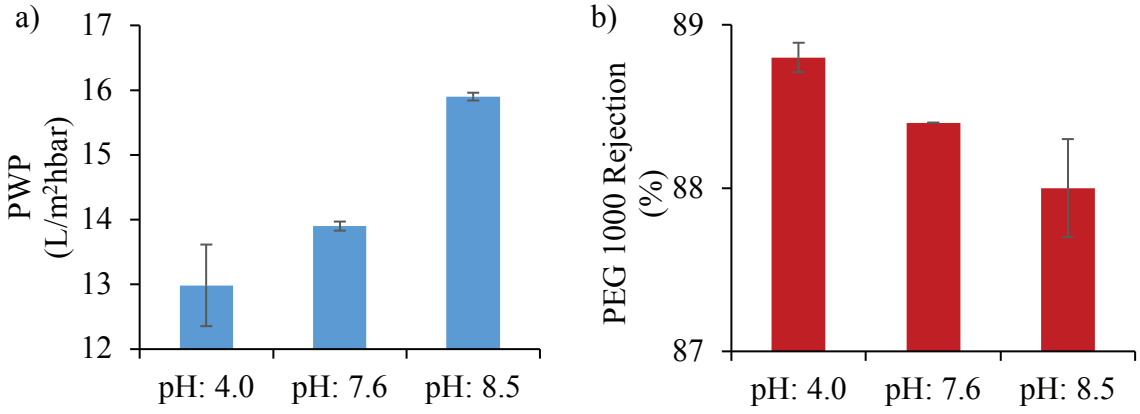

Figure 4.26. Effect of solution pH on a) PWP and b) PEG 1000 rejection of the 25kDa PBC coated membrane.

This is because not only PDEAEM groups in the PBC but also alginate and PEI also display pH dependent degree of protonation. Figure 4.27 illustrates that the PWP of the support and ALG-modified support membranes increased by 1.15 and 1.08 times respectively by increasing pH of water from 4.0 to 8.5. The support membrane was more

significantly influenced by the pH change as a result of again hydrogen bonding between OH ions and amine group in PEI leading to enhanced hydrophilicity of the surface. As seen from Table 4.7, within the experimental error the contact angle of the ALG-modified support membrane remained constant at two pH values while for the support membrane it was 5 degree lower at pH 8.5. With increasing solution pH from 4.0 to 8.5, the support and ALG-modified support rejected 1.34 and 1.07 times higher PEG 1000 molecule, respectively. This is because increasing pH decreases the ionizable groups of PEIs leading to reduction in pore size as a consequence of less repulsion between the chains. On the other hand, ALG is highly charged at pH 8.0 compared to at pH 4.0, thus, makes more charge-charge interaction with excess amine groups of PEIs. As a result, chains respond to the pH change from 4.0 to 8.5 through forming a thinner layer as shown in Figure 4.28. Similar result has been observed by Fulghum et al. (2008). They deposited poly(acrylicacid):poly(allylamine hydrochloride) (PAA:PAH) on a silica support in a layer by layer assembly to produce a pH sensitive ion permeable layer. The highest degree of swelling was observed at pH 3.0 since the carboxylic acid groups in the PAA are less ionized, and the amine functionality in the PAH is more ionized at this pH.

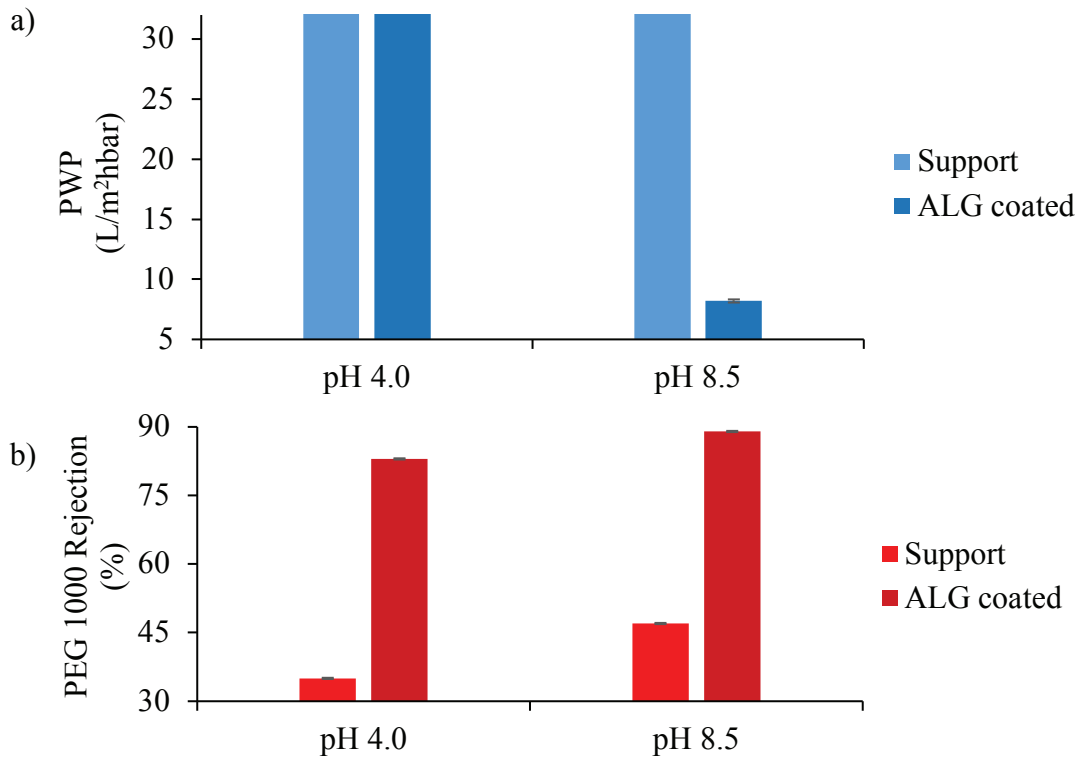

Figure 4.27. Effect of solution pH on a) PWP and b) PEG 1000 rejection of the support and ALG coated membranes.

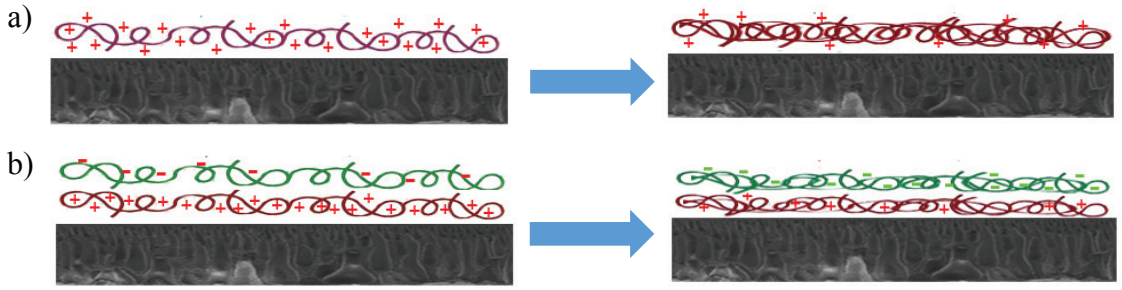

Figure 4.28. pH responsive behavior of support and ALG coated membranes.

In order to observe the pH responsiveness of only PBC, it was adsorbed directly on the support membrane prepared from a blend of PSf and SPES. In this TFC membrane structure other pH responsive polymers, ALG and PEI, do not exist. Figure 4.29 shows the change in PWP, PEG 10000, PEG 6000 and PEG 4000 rejection of the membranes with the pH of feed solution. As seen from the results, the PWP increased while PEG rejection decreased when pH was changed from 4.0 to 8.5. As the solute size becomes smaller, slightly better pH responsiveness on the rejection was observed. Husson and colleagues (Wandera et al., 2010) discussed that at low grafting densities, the responsiveness of the polymer chains approaches to that in solution due to lack of strong interaction between the chains. On other hand, they claimed that responsiveness is weak at high grafting densities since the grafted chains are close to each other which limit their conformational change. In this thesis, the grafting density of PBC was controlled by changing its concentration in the solution. The concentration was limited below the critical micelle concentration of the copolymer to ensure brush-like conformation on the surface. Although all the concentrations studied provided brush conformation, the highest concentration, 18 mg/mL, was chosen to cover pores in the sublayer so that resulting membrane is in NF category. It is clear that direct coating of 25 kDa PBC on the support (the concentration of PBC in solution is 18 mg/mL) resulted in membranes in tight ultrafiltration category. It is possible to increase responsiveness of the chains by decreasing the concentration of PBC in the solution and limit the adsorption time below 12 h which will both lead to lower grafting density compared to the case (adsorption time: 24 h; concentration in solution: 18 mg/mL) shown here.

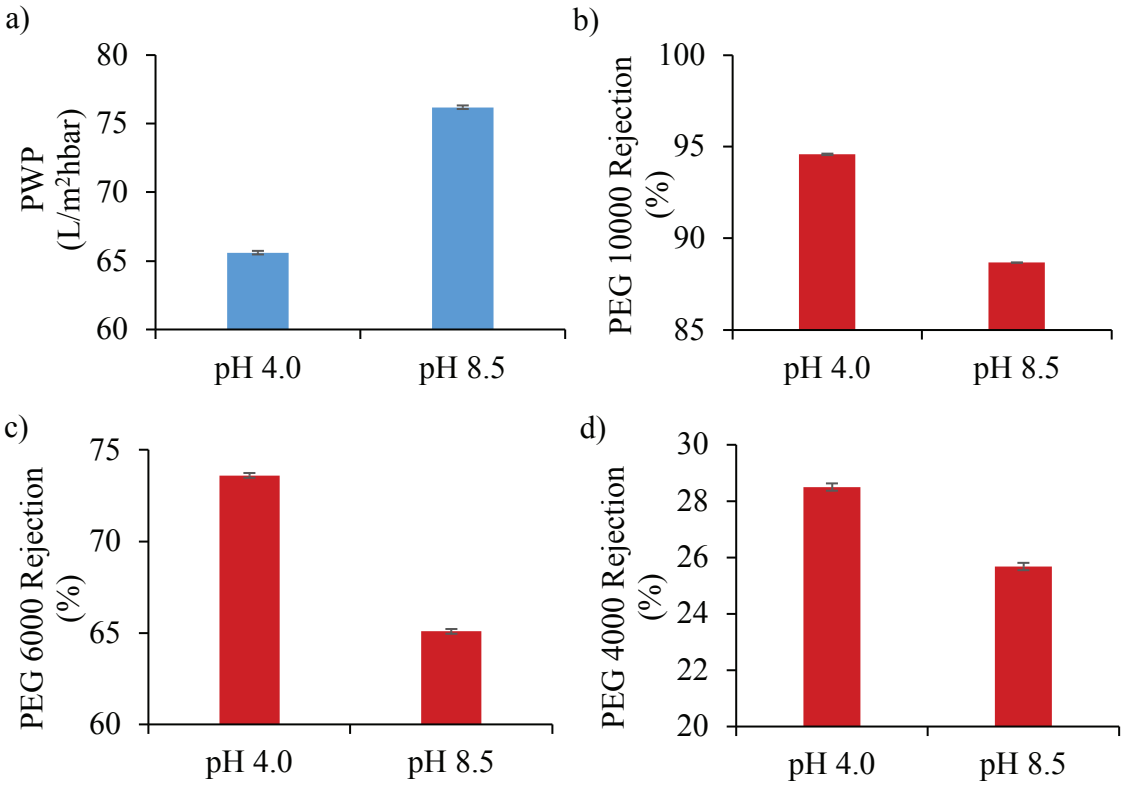

Figure 4.29. Effect of solution pH on the single layer 25 kDa PBC coated membrane performance a) PWP; b) PEG 10000 rejection; c) PEG 6000 rejection; d) PEG 4000 rejections at solution temperature 25°C.

The effect of solution temperature on the permeability and PEG 1000 rejection was illustrated in Figure 4.30. The PBC displays temperature responsiveness due to presence of Pluronic group (PEO-b-PPO-b-PEO). The LCST of the PBC was previously determined as 8°C (Determan et al., 2005). By increasing temperature from 4°C to 25°C higher flux and lower rejection were observed. Below the LCST (4°C), PBC chains become hydrated to form stretched/brush conformation while above the LCST (25°C) chains formed a collapsed/mushroom structure as shown in Figure 4.31. Although the surface is more hydrophilic at 4°C than at 25°C as confirmed by contact angle measurements (Table 4.9), the stretched conformation at 4°C leads to increased mass transfer resistance, hence, lower flux. On the other hand, above the LCST, as the chains contract, the pores are opened, as a result, the PEG 1000 rejection decreased.

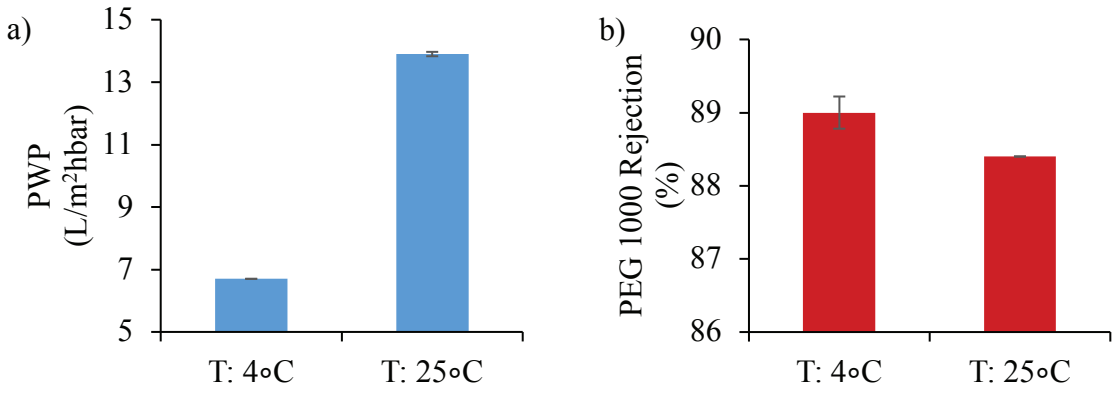

Figure 4.30. Effect of solution temperature on the 25 kDa PBC coated membrane performance at pH 7.6.

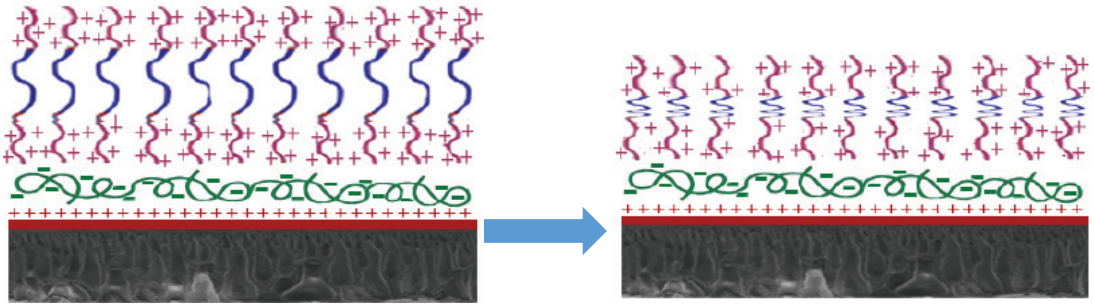

Figure 4.31. Temperature responsive behavior of PBC.

Zhao et al. (2013) examined the temperature responsiveness of the PNIPAAm grafted PVDF membrane from 20 to 44ºC. When the mass ratio of PVDF membrane to NIPAAm was 1:8, the water flux increased from 125 L/m^2 h at 20°C to 155 L/m^2 h at 44°C. This temperature dependent permeability was observed as a result of conformation change of PNIPAAm chains below and above its LCST (around 32°C).

4.6. The Effects of Solution pH and Temperature on MWCO and Average Pore Size of the Membranes

Figure 4.32 show the rejection of different sized solutes by the membrane at different pH and temperature. Figures 4.33 and 4.34 illustrate the change in the MWCO and average pore size of the membranes as a function of filtration pH and temperature. The pore sizes were predicted by combining the rejection data collected with different sized solutes and mathematical model shown in Equations 3.6 to 3.10. The MWCO and

pore size of the membrane at pH 4.0 were 1161 Da and 0.822 nm and the values were altered to 1331 Da and 0.94 nm upon increasing filtration pH to 8.5 (T:25°C). At pH 7.6, when filtration temperature was raised from 4°C (<LCST) to 25°C (>LCST), the MWCO and the pore size of the membrane increased from 1185 Da, 0.826 nm to 1258 Da, 0.891 nm.

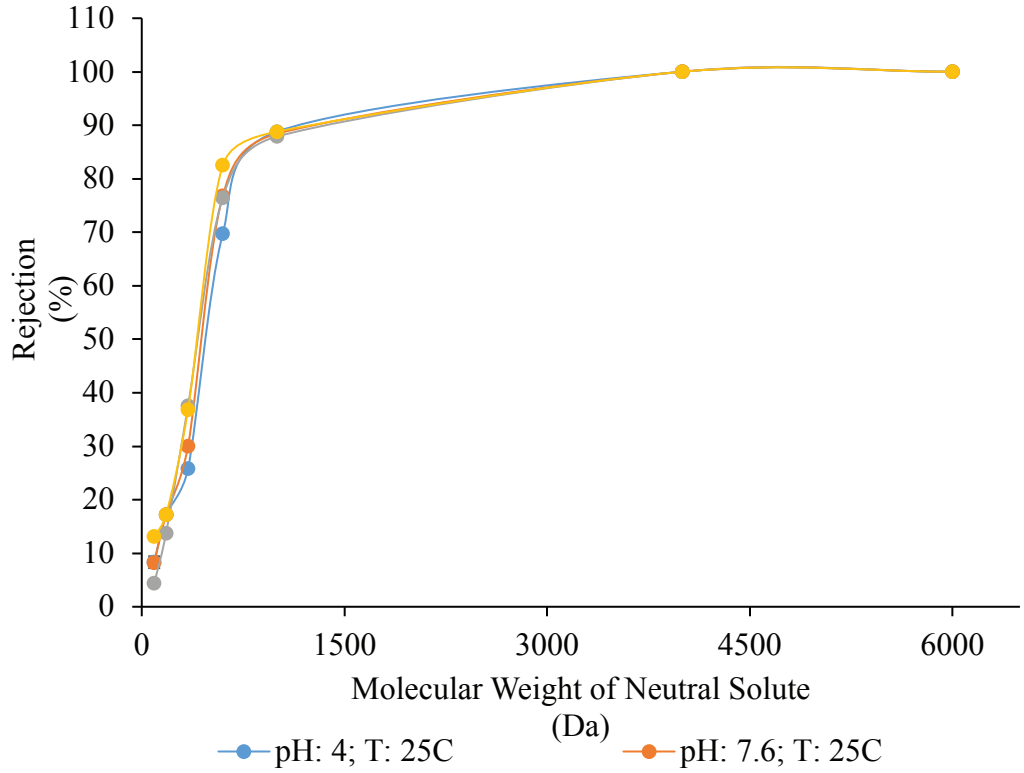

Figure 4.32. MWCO of 25 kDa coated membranes.

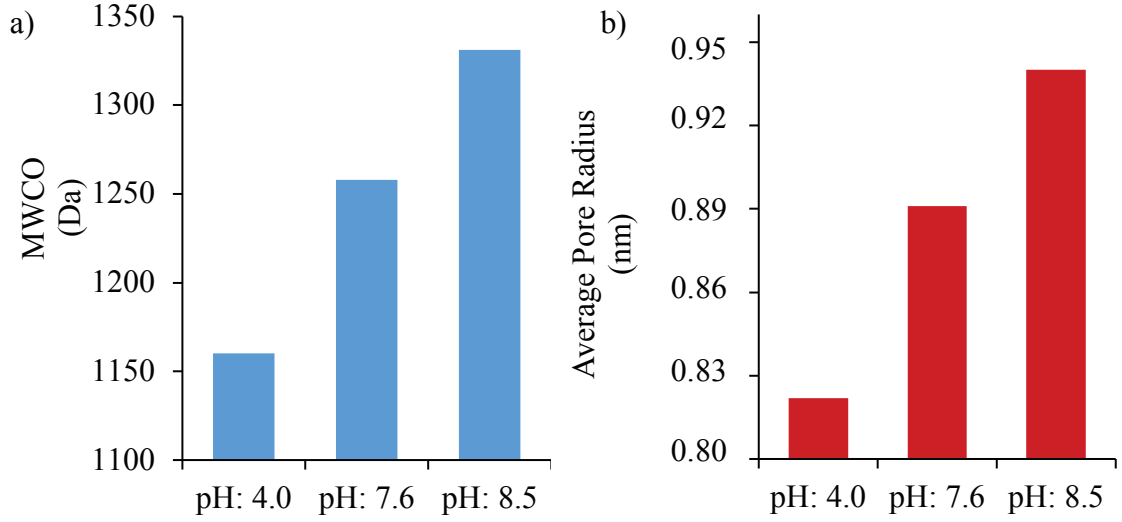

Figure 4.33. Effect of solution pH on the MWCO and average pore radius properties of the 25 kDa PBC coated membrane performance at solution temperature 25°C.

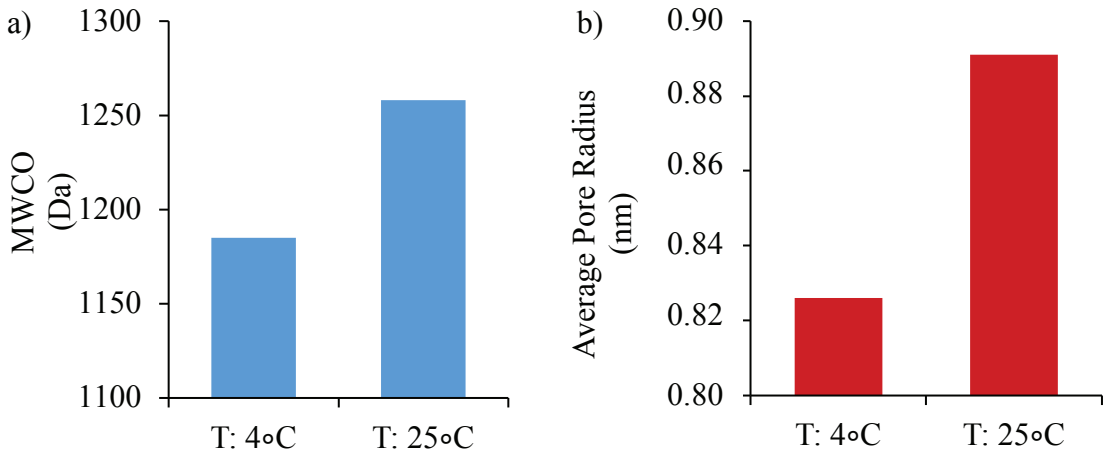

Figure 4.34. Effect of solution temperature on the MWCO and average pore radius properties of the 25 kDa PBC coated membrane performance at solution pH 7.6.

Himstedt et al. (2011) investigated the effect of feed pH on water flux and rejection of glucose as non-ionic solute by modifying the surface of commercial membrane NF270 with acrylic acid to form the nanobrushes. They found that the rejection of glucose was greatest at pH 7.25 above its pKa (4.25) and least at pH 3.15. At pH 7.25 it was expected that these nanobrushes are deprotonated and swollen, hence, pore size was reduced. In another study of Himstedt et al. (2013), PAA nanobrushes were grafted on the surface by UV initiated free radical polymerization method. At constant feed pressure, the flux was reported lower at pH values above pKa of the grafted PAA chains. Glucose rejection was found between 35-45% at pH 3.15 and it increased with increasing pH (55-75% at pH 7.25). Lower flux and higher rejection at pH>pKa was attributed to strong interaction between the negatively charged PAA chains and the solvent water molecules leading to the likely formation of a highly ordered and structured water layer around these negatively charged polymer chains.

Zhao et al. (2013) prepared PVDF support and its average pore diameter was found as 0.960 nm. After surface modification with PNIPAAm, average pore diameter decreased to 0.593 nm. Increasing PNIPAAm amount decreased the average pore diameter as a result of smaller pore formation. Asatekin et al. (2009) studied temperature responsive polymer (PVDF-g-POEM) to adjust pore size by changing environmental conditions. They used Reactive Red 120 (RR) dye solution for rejection experiments. Increasing the temperature increased the amount of RR passed through the membrane. When the temperature approached the LCST, the rejection decreased as a result of pore enlargement.

4.7. Stability of Layers

Stability of the TFC membranes was investigated by storing the membranes in pure water at pH 4.0 and pH 8.5 for 30 days. As seen from the results in Table 4.10, the performance of the membranes both in terms of rejection and PWP slightly changed over 1 month of storage in pH 4.0 and 8.5 which indicated the stability of layers.

Table 4.10. Stability measurement of TFC membranes

	pH 4.0 T 25°C		pH 8.5 T 25°C	
	Storage Time: 0	Storage Time: 30 days	Storage Time: 0	Storage Time: 30 days
PWP (L/m^2hbar)	11 ±0.0	13 ± 0.06	8 ± 0.06	10 ±0.03
PEG 1000 Rejection (%)	85	83	94	90

4.8. Reversibility of pH and Temperature Responsiveness

The reversibility of PWP was determined by alternately switching the solution pH between 4.0 and 8.5 and solution temperature between 4°C and 25°C. The results are shown in Figures 4.35 and 4.36. It can be seen that the permeability immediately changed and was completely reversible upon switching pH and temperature. These results indicated that the conformational change of PBC is reversible.

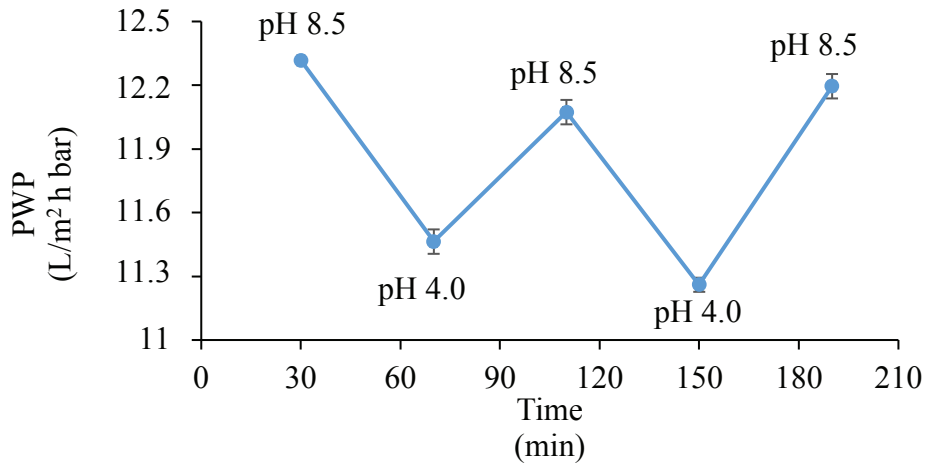

Figure 4.35. Reversible changes of PWP of 25 kDa TFC membrane as a function of pH.

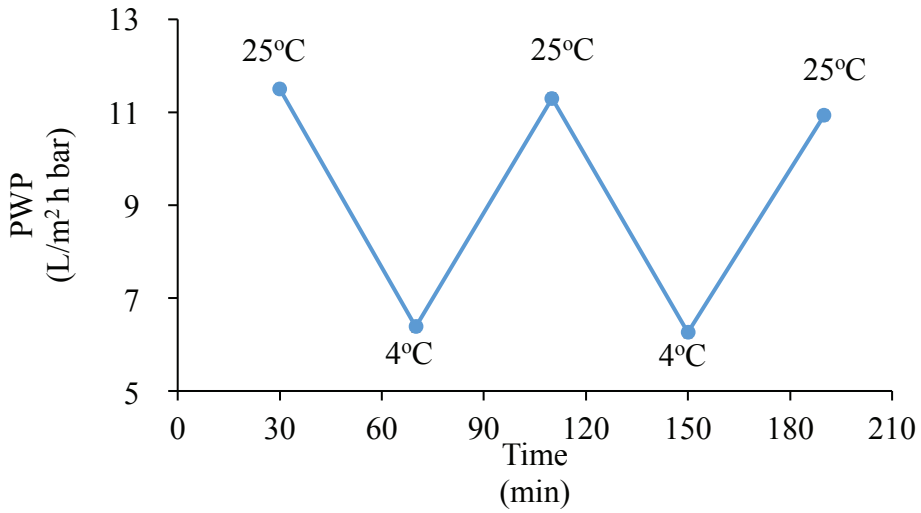

Figure 4.36. Reversible changes of PWP of 25 kDa TFC membrane as a function of temperature.

CHAPTER 5

CONCLUSION

In this thesis, a new stimuli responsive thin film composite NF membrane was developed by coating temperature and pH responsive PBC on the ALG modified PSf:SPES blend membrane. The support with suitable pore size and reasonable permeability (between 20-30 L/m^{2}hbar) was obtained by adding PEI in the coagulation bath. The membranes were characterized in terms of their surface and morphological properties, PWPs, PEG 1000 rejection, pH and temperature responsiveness, layer stabilities and reversibility of PWPs by changing environmental conditions.

SEM, AFM and XPS results have shown that coating was carried out successfully. Regardless of the chain length, maximum grafting density was achieved at the end of 12 h of adsorption. The 25 kDa PBC chains were grafted to the surface in brush conformation at 18 mg/mL. The responsiveness of PBC on the membrane surface was tested by contact angle measurement and filtration experiments. Hydrophilic character of the membrane increased with decreasing temperature on the other hand, contact angle did not significantly change with pH. This is because pH responsiveness of the TFC membrane was influenced not only from PBC but also from ALG and PEI as well. The permeability and selectivity of PBC coated TFC membranes can be tuned by temperature and pH. By adjusting pH and temperature of the feed solution, it is possible to obtain PWP between 12-15 L/m^{2}hbar and PEG 1000 rejection around 90%. MWCO of the membrane changed between 1000 Da and 1300 Da while the pore size ranged from 0.8 nm to 1 nm as a response of the chains to temperature and pH. The membranes displayed good reversible responsiveness and stability in pH range between 4.0 and 9.0. It can be concluded that the stimuli responsive NF membrane developed in this study can have a great potential in the recovery of low molecular weight neutral compounds (<1500 g/mol) even for the fractionation of biomolecules such as peptides through changing the pore size with temperature and pH.

REFERENCES

Algieri, C.; Drioli, E.; Guzzo, L.; Donato, L. Bio-Mimetic Sensors Based on Molecularly Imprinted Membranes. Sensors, **2014**, *14*, 13863-13912.

Alsari, A.M.; Khulbe, K.C.; Matsuura, T. The effect of sodium dodecyl sulfate solutions as gelation media on the formation of PES membranes. Journal of Membrane Science, **2001**, *188*, 279-293.

Amirilargani, M.; Saljoughi, E.; Mohammadi, T.; Moghbeli, M.R. Effects of Coagulation Bath Temperature and Polyvinylpyrrolidone Content on Flat Sheet Asymmetric Polyethersulfone Membranes. Polymer Engineering & Science, **2010**, *50*, 885-893.

Arya, R.K. Drying Induced Phase Separation. Journal of Chemical Engineering, **2012**, *27*, 12-20.

Asatekin, A.; Mayes, A.M. Responsive pore size properties of composite NF membranes based on PVDF grafted copolymers. Separation Science and Technology, **2009**, *44*, 3330-3345.

Bellona, C.; Drewes, J.E.; Xu, P.; Amy, G. Factors affecting the rejection of organic solutes during NF/RO treatment-a literature review. Water Research, **2004**, *38*, 2795-2809.

Berndt, E.; Ulbricht, M. Synthesis of block copolymers for surface functionalization with stimuli-responsive macromolecules. Polymer, **2009**, *50*, 5181-5191.

Birkner, M.; Ulbricht, M. Ultrafiltration membranes with markedly different pH- and ion-responsivity by photografted zwitterionic polysulfobetain or polycarbobetain. Journal of Membrane Science, **2015**, *494*, 57-67.

Boussu, K.; Vandecasteele, C.; Van der Bruggen, B. Study of the characteristics and the performance of self-made nanoporous polyethersulfone membranes. Polymer, **2006**, *47*, 3464-3476.

Boussu, K.; Van der Bruggen, B.; Volodin, A.; Van Haesendonck, C.; Delcour, J.A.; Van der Meeren, P.; Vandecasteele, C. Characterization of commercial nanofiltration membranes and comparison with self-made polyethersulfone membranes. Desalination, **2006**, *191,* 245-253.

Bowen, W.R.; Mohammad, A.W. Characterization and prediction of nanofiltration membrane performance-A general assessment. I. Chem. E., **1998**, *76*, 885-893.

Chen, Y.C.; Xie, R.; Chu, L.Y. Stimuli-responsive gating membranes responding to temperature, pH, salt concentration and anion species. J. Membr. Sci., **2013**, *442*, 206-215.

Chen, X.; Zhao, B.; Han, P.; Fu, W.; Chen, L. Temperature- and pH-sensitive membrane formed from blends of poly(vinylidene fluoride)-graft-poly(N-isopropylacrylamide) and poly(acrylic acid) microgels. Reactive and Functional Polymer, **2014**, *84*, 10-20.

Chen, X.; He, Y.; Shi, C.; Fu, W.; Bi, S.; Wang, Z.; Chen, L. Temperature- and pH-responsive membranes based on poly (vinylidene fluoride) functionalized with microgels. Journal of Membrane Science, **2014**, *469*, 447-457.

Cheryan, M. Ultrafiltration and Microfiltration Handbook. Lancaster, PA.: economic Publishing Co., Inc., **1998**.

Dan, N.; Tirrell, M. Self-Assembly of Block Copolymers with a Strongly Charged and a Hydrophobic Block in a Selective, Polar Solvent-Micelles and Adsorbed Layers. Macromolecules, **1993**, *26*, 4310-4315.

Davrishmanesh, S.; Qian, X.; Wickramasinghe, S.R. Responsive membranes for advanced separations. Current Opinion in Chemical Engineering, **2015**, *8*, 98-104.

Deen, W.M. Hindered transport of large molecules in liquid-filled pores. AlChE Journal, **1987**, *33*, 1409-1425.

Determan, M.D.; Guo, L.; Thiyagarajan, P.; Mallapragada, S.K. Supramolecular self-assembly of multiblock copolymers in aqueous solution. Langmuir, **2006**, *22*, 1469-1473.

Determan, M.D.; Cox, J.P.; Seifert, S.; Thiyagarajan, P.; Mallapragada, S.K. Synthesis and characterization of temperature and pH-responsive pentablock copolymers. Polymer. **2005**, *46*, 6933–6946.

Guillen, G.R.; Pan, Y.; Li, M.; Hoek, E.M.V. Preparation and Characterization of Membranes Formed by Nonsolvent Induced Phase Separation: A Review. Ind. Eng. Chem. Res., **2011**, *50*, 3798–3817.

Hammouda, B. Temperature effect on the nanostructure of SDS micelles in water. Journal of Research of the National Institute of Standards and Technology, **2013**, *118*, 151-167.

He, Y.; Chen, X.; Bi, S.; Shi, C.; Chen, L., Li, L. Structure and pH-sensitive properties of poly (vinylidene fluoride) membrane changed by blending poly (acrylic acid) microgels. Polym. Adv. Technol., **2013**, *24*, 934-944.

Himstedt, H.H.; Marshall, K.M.; Wickramasinghe, S.R. pH-responsive nanofiltration membranes by surface modification. Journal of Membrane Science, **2011**, *366*, 373-381.

Himstedt, H.H.; Du, H.; Marshall, K.M.; Wickramasinghe, S.R.; Qian, X. pH-responsive nanofiltration membranes for sugar separation. Ind. Eng. Chem. Res., **2013**, *52*, 9259-9269.

Jacob, K.N.; Kumar, S.S.; Thanigaivelan, A.; Tarun, M.; Mohan, D. Sulfonated polyethersulfone-based membranes for metal ion removal via a hybrid process. Journal of Material Science, **2014**, *49*, 114-122.

Jamil, S.M.; Othman, M.H.D.; Rahman, M.A.; Jaafar, J.; Ismail, A.F.; Li, K. Recent fabrication techniques for micro-tubular solid oxide fuel cell support: A review. Journal of the European Ceramic Society, **2015**, *35*, 1-22.

Lau, W.J.; Ismail, A.F.; Misdan, N.; Kassim, M.A. A recent progress in thin film composite membrane: a review. Desalination, **2012**, *287*, 190–199.

Lee, H.; Pietrasik, J.; Sheiko, S.S.; Matyjaszewski, K. Stimuli-responsive molecular brushes. Progress in Polymer Science, **2010**, *35,* 24-44.

Li, H.; Liao, J.; Xiang, T.; Wang, R.; Wang, D.; Sun, S.; Zhao, C. Preparation and characterization of pH- and thermos-sensitive polyethersulfone hollow fiber membranes modified with P(NIPAAm-MAA-MMA) terpolymer. Desalination, **2013**, *309*, 1-10.

Liangyin C.; Rui X.; Xiaojie J. Stimuli-responsive Membranes: Smart Tools for Controllable Mass-transfer and Separation Processes. Chinese Journal of Chemical Engineering, **2011,** *19*, 891-903.

Lin, Y.; Alexandridis, P. Temperature-Dependent Adsorption of Pluronic F127 Block Copolymers onto Carbon Black Particles Dispersed in Aqueous Media. J. Phys. Chem. B., **2002**, *42*, 10834-10844.

Liu, M.M.; Zhao, L.Z.; Li, S.S.; Ye, H.; An, H.Q.; Zhang, Y.Z. pH-responsive ethylene alcohol copolymer membrane based on porphyrin supramolecular self-assembly. RSC Adv., **2016**, *6*, 10704-10712.

Liu, F.; Urban, M.W. Recent advances and challenges in designing stimuli-responsive polymers. Progress in Polymer Science, **2010***, 35*, 3-23.

Marcel, M. *Basic Principles of Membrane Technology*, 2nd ed.; Dordrecht: Kluwer Academic Publishers: Boston, **1996**.

Ulbricht, M. Advanced functional polymer membranes. Polymer, **2006**, *47*, 2217-2262.

Mohsenpour, S.; Esmaeilzadeh, F.; Safekordi, A.; Tavakolmoghadam, M.; Rekabdar, F.; Hemmati, M. The role of thermodynamic parameter on membrane morphology based on phase diagram. Journal of Molecular Liquids, **2016**, *224*, 776-785.

Mulvenna, R.A.; Weidman, J.L.; Jing, B.; Pople, J.A.; Zhu, Y.; Boudouris, B.W.; Phillip, W.A. Tunable nanoporous membranes with chemically-tailored pore walls from triblock polymer templates. Journal of Membrane Science, **2014**, *470*, 246-256.

Nguyen*,* Q.T.; Glinel, K.; Pontié, M.; Ping, Z. Immobilization of bio-macromolecules onto membranes via an adsorbed nanolayer An insight into the mechanism. Journal of Membrane Science, **2004**, *232*, 123–132.

Nunes, S.P.; Behzad, A.R.; Hooghan, B.; Sougrat, R.; Karunakaran, M.; Pradeep, N.; Vainio, U.; Peinemann, K. Switchable pH-responsive polymeric membranes prepared via block copolymer micelle assembly. ACS Nano, **2011**, *5*, 3516-3522.

Pinto, C.G.; Laespada, M.E.F.; Pavón, J.L.P.; Cordero, B.M. Analytical applications of separation techniques through membranes. Laboratory Automation & Information Management, **1999**, *34*, 115-130.

Shevate, R.; Karunakaran, M.; Kumar, M.; Peinemann, K. Polyanionic pH-responsive polystyrene-b-poly(4-vinyl pyridine-N-oxide) isoporous membranes**.** J. Membr. Sci., **2016,** *501*, 161-168.

Thong, Z.; Han, G.; Cui, Y.; Gao, J.; Chung, T.S.; Chan, S.Y.; Wei, S. Novel Nanofiltration Membranes Consisting of a Sulfonated Pentablock Copolymer Rejection Layer for Heavy Metal Removal. Environ. Sci. Technol., **2014**, *48*, 13880-13887.

Tomer, N.; Mondal, S.; Wandera, D.; Wickramansinghe, S.R.; Husson, S.M. Modification of Nanofiltration Membranes by Surface-Initiated Atom Transfer Radical Polymerization for Produced Water Filtration. Separation Science and Technology, **2009**, *44*, 3346-3368.

Tomicki, F.; Krix, D.; Nienhaus, H.; Ulbricht, M. Stimuli–responsive track-etched membranes via surface-initiated controlled radical polymerization: Influence of grafting density and pore size. Journal of Membrane Science, **2011**, *377*, 124-133.

Van der Bruggen, B.; Vandecasteele, C.; Van Gestel, T.; Doyen, W.; Leysen, R. A Review of Pressure-Driven Membrane Processes in Wastewater Treatment and Drinking Water Production. Environmental Progress, **2003**, *22*, 46-56.

Wandera D.; Wickramasinghe S.R.; Husson S.M. Stimuli-responsive membranes. Journal of Membrane Science, **2010**, *357*, 6-35.

Wang, M.; Yan, F.; Zhao, L.; Zhang, Y.; Sorci, M. Preparation and characterization of a pH-responsive membrane carrier for meso-tetraphenylsulfonato porphyrin. RSC Adv., **2017**, *7*, 1687-1696.

Wu, C.; Zhao, L.; Zhang, Y. pH-Responsive nanofiltraiton membranes based on porphyrin supramolecular self-assembly by layer-by-layer technique. RSC Advances, **2017**, *7*, 47397-47406.

Xiao, L.; Isner, A.; Waldrop, K.; Saad, A.; Takigawa, D.; Bhattacharyya, D. Development of bench and full-scale temperature and pH responsive functionalized PVDF membranes with tunable properties. Journal of Membrane Science, **2014**, *457*, 39-49.

Yang, B.; Yang, X.; Liu, B.; Chen, Z.; Chen, C.; Liang, S.; Chu, L.-Y.; Crittenden, J. PVDF blended PVDF-g-PMAA pH-responsive membrane: Effect of additives and solvents on membrane properties and performance. Journal of Membrane Science, **2017**, *541*, 558-566.

Yang, Q.; Himstedt, H.H.; Ulbricht, M.; Qian, X.; Wickramasinghe, S.R. Designing magnetic field responsive nanofiltration membranes. Journal of Membrane Science, **2013**, *430*, 70-78.

Yi, Z.; Zhu, L.P.; Xi, Y.Y.; Li, X.L.; Yu, J.Z.; Zhu, B.K. F127-based multi-block copolymer additives with poly(N,N-dimethylamino-2-ethyl methacrylate) end chains: The hydrophilicity and stimuli-responsive behavior investigation in polyethersulfone membranes modification. Journal of Membrane Science, **2010**, *364*, 34-42.

Zhao, X.; Zhang, Z.; Pan, F.; Ma, Y.; Armes, S.P.; Lewis, A.L.; Lu, J.R. Solution pH-Regulated Interfacial Adsorption of Diblock Phosphorylcholine Copolymers. Langmuir, **2005**, *21*, 9597-9603.

Zhao, Y.; Zhao, H.; Chen, L.; Feng, X.; Zhang, Q.; Wang, J.; Zhang, R. Thermo-responsive modification and properties study of PVDF flat membrane. J. Polym. Res., **2013**, 20-58.

Zhou, T.; Qi, H.; Han, L.; Barbash, D.; Li, C.Y. Towards controlled polymer brushes via a self-assembly-assisted-grafting-to approach. Nature Communications, **2016**, *7*, 11119.

Zhu, Y.; Wang, D.; Jiang, L.; Jin, J. Recent progress in developing advanced membranes for emulsified oil/water separation. NPG Asia Materials, **2014**, *6*, 1-11.